cells

Article

Residual Cystine Transport Activity for Specific Infantile and Juvenile *CTNS* Mutations in a PTEC-Based Addback Model

Louise Medaer [1], Dries David [1], Maxime Smits [1,2], Elena Levtchenko [3,4], Maurilio Sampaolesi [5] and Rik Gijsbers [1,2,*]

1 Laboratory of Molecular Virology and Gene Therapy, Department of Pharmacological and Pharmaceutical Sciences, Faculty of Medicine, KU Leuven, 3000 Leuven, Belgium; louise.medaer@kuleuven.be (L.M.); maxime.smits@kuleuven.be (M.S.)
2 Leuven Viral Vector Core, Faculty of Medicine, KU Leuven, 3000 Leuven, Belgium
3 Department of Paediatric Nephrology & Development and Regeneration, University Hospitals Leuven & KU Leuven, 3000 Leuven, Belgium; e.n.levtchenko@amsterdamumc.nl
4 Department of Paediatric Nephrology, Amsterdam University Medical Centre, 1081 Amsterdam, The Netherlands
5 Translational Cardiology Laboratory, Department of Development and Regeneration, Stem Cell Institute, Faculty of Medicine, KU Leuven, 3000 Leuven, Belgium; maurilio.sampaolesi@kuleuven.be
* Correspondence: rik.gijsbers@kuleuven.be; Tel.: +32-16-37-48-41

Abstract: Cystinosis is a rare, autosomal recessive, lysosomal storage disease caused by mutations in the gene *CTNS*, leading to cystine accumulation in the lysosomes. While cysteamine lowers the cystine levels, it does not cure the disease, suggesting that CTNS exerts additional functions besides cystine transport. This study investigated the impact of infantile and juvenile *CTNS* mutations with discrepant genotype/phenotype correlations on CTNS expression, and subcellular localisation and function in clinically relevant cystinosis cell models to better understand the link between genotype and CTNS function. Using CTNS-depleted proximal tubule epithelial cells and patient-derived fibroblasts, we expressed a selection of CTNS^{mutants} under various promoters. *EF1a*-driven expression led to substantial overexpression, resulting in CTNS protein levels that localised to the lysosomal compartment. All CTNS^{mutants} tested also reversed cystine accumulation, indicating that CTNS^{mutants} still exert transport activity, possibly due to the overexpression conditions. Surprisingly, even CTNS^{mutants} expression driven by the less potent *CTNS* and *EFS* promoters reversed the cystine accumulation, contrary to the CTNS^{G339R} missense mutant. Taken together, our findings shed new light on *CTNS* mutations, highlighting the need for robust assessment methodologies in clinically relevant cellular models and thus paving the way for better stratification of cystinosis patients, and advocating for the development of more personalized therapy.

Keywords: cystinosis; kidney disease; CTNS^{mutants}; gene therapy; viral vectors

Citation: Medaer, L.; David, D.; Smits, M.; Levtchenko, E.; Sampaolesi, M.; Gijsbers, R. Residual Cystine Transport Activity for Specific Infantile and Juvenile *CTNS* Mutations in a PTEC-Based Addback Model. *Cells* **2024**, *13*, 646. https://doi.org/10.3390/cells13070646

Academic Editor: Ritva Tikkanen

Received: 10 March 2024
Revised: 3 April 2024
Accepted: 4 April 2024
Published: 6 April 2024

1. Introduction

Cystinosis is a monogenic, autosomal recessive, lysosomal storage disease caused by biallelic mutation in the *CTNS* gene (17p13.2) [1–3]. This gene encodes cystinosin (CTNS, 367 AA), a H^+-cystine symporter transporting cystine to the cytosol (Figure 1) [4,5]. It includes seven transmembrane (TM) domains with seven predicted N-glycosylation sites at the N-terminus, and lysosomal targeting motifs located at the C-terminus (GYDQL) and the PQ-loop in the fifth inter-transmembrane (IT) region (YFPQA). *CTNS* mutations are shown to cause a defect in the CTNS cystine transport activity and thus lead to an accumulation of cystine in the lysosomes of all body cells and tissues, making cystinosis a systemic disease with the kidney and the eyes being the first organs to be affected [6–9]. In the clinic, three phenotypes are distinguished: nephropathic infantile, nephropathic juvenile, and non-nephropathic ocular cystinosis [10]. Patients with nephropathic infantile cystinosis (OMIM 219800) appear normal at birth but early clinical manifestations (around

6–9 months of age) include a failure to thrive and rickets because of the generalized dysfunction of kidney proximal tubule cells (PTECs), also called renal Fanconi syndrome. If left untreated, infantile cystinosis leads to end-stage kidney disease (ESKD) by the age of 10 [11–13]. In the case of nephropathic juvenile cystinosis (OMIM 219900), patients are diagnosed later in childhood or during adolescence, with milder forms of the renal Fanconi syndrome or isolated proteinuria with a slower rate of progression towards ESKD [13–15]. The non-nephropathic ocular phenotype (OMIM 21975), diagnosed in adults, is mild and characterized photophobia due to cystine accumulation in the cornea and conjunctiva of the eyes without systemic organ damage [10,12,16]. For treating cystinosis, the beneficial role of cysteamine therapy has been well described for nearly four decades. Although it does not reverse proximal tubulopathy, it considerably delays progression towards kidney failure and postpones non-renal complications [17,18].

To date, over 165 mutations have been reported for cystinosis, which include 69 missense and nonsense mutations, 23 splicing mutations, 52 deletions, 15 insertions, four indels, and two promoter region mutations [19,20]. The most common pathogenic mutation, representing approximately 50% of mutant alleles in the Caucasian population, is a 57-kb deletion encompassing the *CTNS* promoter together with the first nine exons and part of exon 10 together with the gene *CARKL* and the first two non-coding exons of *TRPV1* upstream of *CTNS* [14,21–23]. The effect of *CTNS* missense mutations and small indels on protein expression, subcellular distribution, and function is only poorly understood, and has been primarily studied in overexpression conditions (transient transfection) with CTNS proteins carrying an outspoken eGFP tag (27 kDa), and mostly in non-human cell lines [24–27]. Moreover, to assess transport activity, CTNS was reengineered by removing the C-terminal lysosomal targeting motif GYDQL to redirect CTNS and CTNS mutant proteins to the plasma membrane (PM) [26]. Recently, the crystal structures of *Homo sapiens* and *Arabidopsis thaliana* CTNS were solved in lumen-open, cytosol-open, and cystine-bound states by crystallography and cryo-EM, revealing the cystine recognition mechanism and key conformational states of the proton-coupled transport cycle [27,28]. These studies, together with Alphafold and AlphaMissense provided us with a framework for a better understanding of the genotype–phenotype interplay, allowing us to explore the impact of missense mutations causing cystinosis on CTNS' function [29,30].

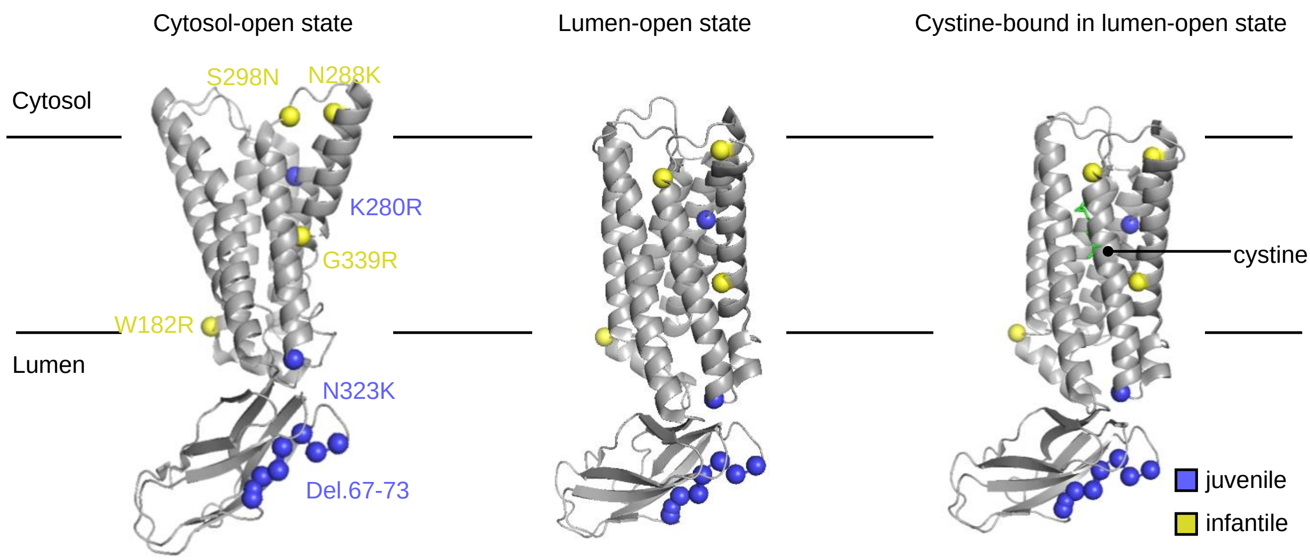

(A)

Figure 1. *Cont.*

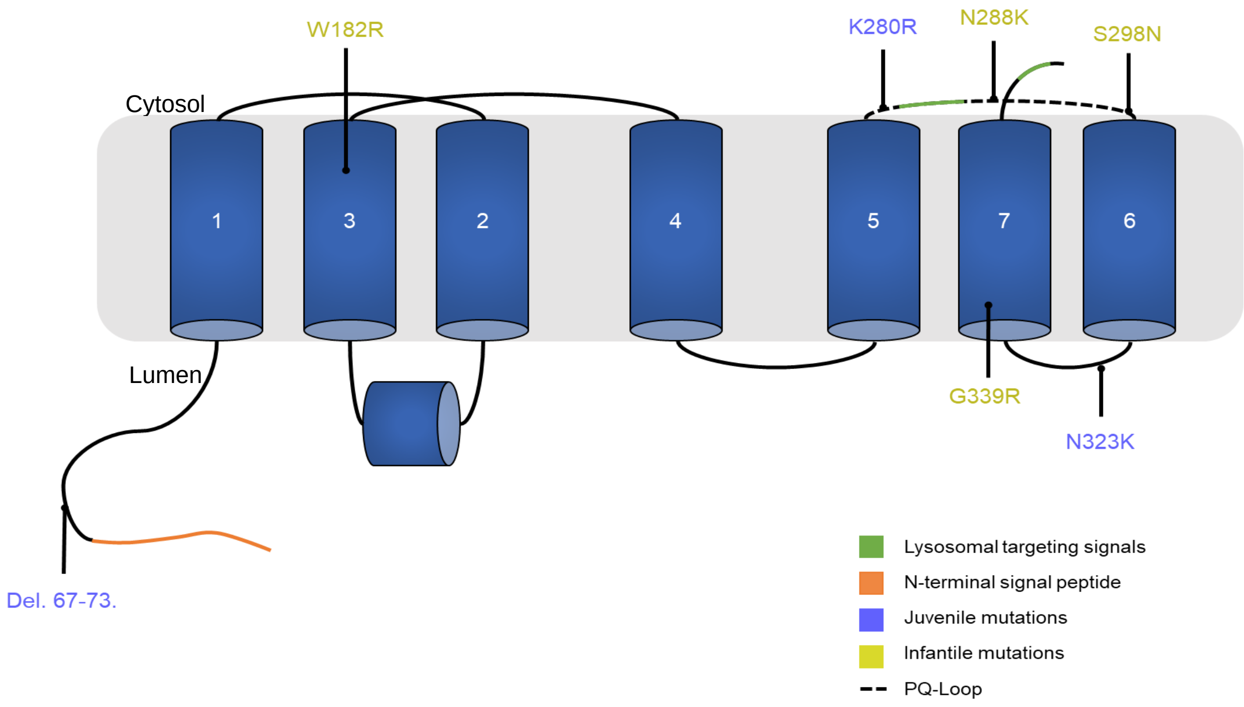

(**B**)

Figure 1. Schematic overview of the CTNS protein with the mutations studied annotated. (**A**) Cryo-EM structures of CTNS in cytosol-open (8DKE), lumen-open (8DKI), and cystine-bound lumen-open (8DKM) state. Mutations are shown in spheres and coloured by clinical phenotypes. Structures indicated were viewed with PyMol 2.4.1. (**B**) Topology of CTNS with mutations indicated and coloured by clinical phenotypes.

In this study, we set out to determine the effect of specific point mutations and expression levels on CTNS activity in a clinically relevant kidney-derived proximal tubule cell model using stable lentiviral vector (LV)-mediated expression. We studied a subset of CTNS missense mutations and a small deletion that causes either infantile or juvenile phenotypes in patients living with cystinosis with discrepant genotype/phenotype correlations, and assessed expression, subcellular location, and cystine accumulation at different expression levels.

2. Materials and Methods

2.1. Cell Culture

The conditionally immortalized proximal tubulus epithelial cells (ciPTECs) cell lines used in this study are the following: a healthy control ciPTEC 14.4 cell line (referred to as *CTNS*$^{+/+}$) and a CTNS-depleted ciPTEC cell line (referred to as *CTNS*$^{-/-}$) derived from ciPTEC 14.4. ciPTECs 14.4 were generated by the isolation of PT cells obtained from urine from healthy volunteers and transfected with a temperature-sensitive mutant U19tsA58 of SV40 large T antigen (SV40T) and the essential catalytic subunit of human telomerase as described earlier [31]. *CTNS*$^{-/-}$ ciPTECs were described earlier (kind gift from Dr. Janssen M. and Prof. Masereeuw R., Utrecht University, the Netherlands) [32]. *CTNS*$^{-/-}$ ciPTEC is an isogenic clone derived from ciPTEC 14.4 and generated using CRISPR-Cas9, which harbors a 13-base pair (bp) and 85 bp deletion in exon 4 of the *CTNS* gene. The cells were cultured in Dulbecco's modified Eagle DMEM F-12 (L0093-500; Biowest, Leuven, VWR Belgium) supplemented with 5 mL/500 mL insulin–transferrin–selenium (I-1884; Sigma, Overijse, Belgium), 36 ng/mL hydrocortisone (Sigma, H0135), 10 ng/mL EGF (E9644; Sigma, Overijse, Belgium), 40 pg/mL tri-iodothryonine (T5516, Sigma, Overijse, Belgium), 10% fetal bovine serum (*v*/*v*; DE17-602E; Biowest, Leuven, VWR Belgium), and

1.1% Pen/Strep (DE17-602E; Westburg, Leusden, The Netherlands) [32]. After transduction, the cells were selected with puromycin (1 µg/mL; ant-pr-1; Invivogen, Toulouse, France). ciPTECs were grown at 33 °C and 5% (*v*/*v*) CO_2 for proliferation up to 90% confluency and matured into differentiated epithelial cells by culturing at 37 °C for 7 days [31].

The Fcys (*CTNS*$^{-/-}$; Fcys32) fibroblast cell line, isolated from skin samples of a cystinosis patient, was developed as described earlier [33,34]. The genotype consists of a homozygous 57 kb deletion of the *CTNS* gene. The FCo (*CTNS*$^{+/+}$; FCo5) control fibroblast cell line was derived from a healthy volunteer [33,34]. The cells were cultured in DMEM/F-12 medium (Invitrogen, Merelbeke, Belgium), supplemented with 10% fetal bovine serum (*v*/*v*; DE17-602E; Biowest, Leuven, VWR Belgium), L-glutamine (4 mM, Invitrogen, Merelbeke, Belgium), penicillin (100 U/mL; Invitrogen, Merelbeke, Belgium), and streptomycin (100 µg/mL; Invitrogen, Merelbeke, Belgium). The fibroblasts were grown at 37 °C and 5% (*v*/*v*) CO_2 for proliferation.

2.2. Generation of LV Transfer Plasmids for *CTNS*^{WT} or *CTNS*^{mutants}

The human *CTNS*^{WT}, *CTNS*^{mutants}, *eGFP*, and *dATP13A2* cDNA were cloned in the self-inactivating lentiviral (SIN-LV) backbone plasmid pCH-promoter-X-IRES-PuroR-WPRE (Didier Trono) using Gblocks at the BcuI and Bsp119I4 restriction sites. The cDNA constructs encoding eGFP and dATP13A2 (D508N), a catalytically dead version of ATP13A2, a lysosomal transmembrane protein, were used as transduction controls and to control for overexpression. The vector backbone contained one of the following promoters: *CMV-*, *EF1a*, *EFS* (EF1a short), or *CTNS* promoter [35,36]. The *CTNS*$^{WT/mutant}$ cDNA was tagged with a triple hemagglutinin tag (3HA tag) at its C-terminus.

2.3. Production of LV Vectors and Generation of Stable Cell Lines Expressing *CTNS*^{WT} or *CTNS*^{mutants} Driven by Different Promoters

LVs were produced as previously reported [37]. Functional validation of the LV_CTNS^{WT}-3HA constructs was reported in Veys et al. [38]. To ensure a single integrated viral vector copy per cell, viral vector transduction was conducted employing a limiting dilution series. Cells were seeded in a 96-well plate to reach the ideal confluency at 10,000 cells, grown overnight, and transduced with the respective LV vector preparations. A total of 72 h later, the medium was replaced with puromycin-containing (1 µg/mL, ant-pr-1; Invivogen, Toulouse, France) medium to select transduced cells. To ensure a single integrated viral vector copy, we selected the highest dilution that still resulted in surviving cells upon puromycin selection (<20% transduced cells, MOI < 0.5) [39].

2.4. Determination of Integrated Copies

gDNA was extracted using the GenElute™ Mammalian Genomic DNA miniprep Kit (Sigma, Overijse, Belgium) according to the manufacturer's protocol. A total of 25 ng/µL gDNA was used for qPCR to determine integrated copies based on the woodchuck hepatitis virus post-transcriptional regulatory element (WPRE). As a control, a single integrated copy control (1ICC) was made generated by transducing HEK293T cells in a limiting dilution series with an LV expressing pEF1a-CTNS^{WT}-eGFP-IRES-PuroR. Cells were monitored by flow cytometry analysis, and the condition where the Mean Fluorescence Intensity (MFI) did not drop when the vector was diluted, but the % eGFP positive cells did, was considered as the 1ICC condition. Following puromycin selection, the highest dilution that survived the selection was chosen. RT-qPCR was performed using 25 ng/µL gDNA, dsDNA-intercalating agent LightCycler® 480 SYBR Green I (Roche Life Science, Brussels, Belgium), and 10 µM primers (see Table S1). RT-qPCR was performed on the CFX Opus 96 Real-Time PCR instrument (Bio-Rad, Temse, Belgium) and data were retrieved and analysed using the CFX maestro 2.2 software. Amplification was performed for 50 cycles of 10 s at 95 °C and 30 s at 60 °C. The fold change was calculated as fold change = $2^{-\Delta\Delta Ct}$.

2.5. Quantification of CTNS-3HA mRNA Expression Levels

Total mRNA was extracted using the AurumTM Total RNA Mini Kit (Bio-rad, Temse, Belgium) following the manufacturers' instructions. cDNA was synthesized from the extracted mRNA samples using the High-Capacity cDNA Reverse Transcription Kit (Applied Biosystems, Merelbeke, Belgium). RT-qPCR was performed using 5 ng/µL cDNA, dsDNA-intercalating agent LightCycler® 480 SYBR Green I (Roche Life Science, Brussels, Belgium), and 10 µM primers. Primers were designed to land in exonic sequences, spanning exon 10 and 11, allowing for the assessment of endogenous mRNA- and LV-expressed *CTNS* mRNA (Table S1). RT-qPCR was performed on the CFX Opus 96 Real-Time PCR instrument (Bio-Rad, Temse, Belgium) and data were retrieved and analysed using the CFX maestro 2.2 software. Amplification was performed for 50 cycles of 10 s at 95 °C and 30 s at 60 °C. The fold change was calculated as fold change = $2^{-\Delta\Delta Ct}$.

2.6. Metabolite and Cystine Measurements

The ciPTECs were seeded at 55,000 cells/cm^2 in a 6-well plate and allowed to differentiate at 37 °C for 7 days. Samples were prepared by removing the medium and washing the cells with a 0.9% NaCl solution. The washing solution was removed and the extraction buffer was added. The extraction buffer with cystine internal standard is prepared as follows. A 20 mM $^{15}N_2$-Cystine stock standard was prepared by dissolving 4.8 mg $^{15}N_2$-cystine (Cambridge Isotope Laboratories NLM-3818; Apeldoorn, The Netherlands) in 1 mL of a 30/70 volume ratio mix of respectively, 2M HCl (fuming 37%, 1.00317.1000 Merck, Hoeilaart, Belgium) in milliQ water and methanol (85800.320; VWR, Leuven, Belgium). This solution was then diluted to insert the final concentration in a solution of 80/20 methanol/milliQ water with 0.1 v% formic acid (85048.001; VWR, Leuven, Belgium). Using a cell scrape, the extract was transferred into an Eppendorf tube. Proteins were pelleted by centrifugation for 15 min at 20,000× *g* at 4 °C and used to normalization, determined by a Pierce™ BCA protein assay (Thermo Scientific, Dilbeek, Belgium). The supernatant was transferred to a new Eppendorf to perform mass spectrometry. Mass spectrometry measurements were performed using a Vanquish LC System (Thermo Scientific, Dilbeek, Belgium) coupled via heated electrospray ionization to a Q Exactive Orbitrap Focus mass spectrometer (Thermo Scientific, Dilbeek, Belgium). A 10 µL sample was taken from an MS vial and injected onto a Poroshell 120 HILIC-Z PEEK Column (Agilent InfinityLab, Zaventem, Belgium). A linear gradient was carried out starting with 90% solvent A (acetonitrile with 5 µM medronic acid) and 10% solvent B (10 mM NH_4-formate in milli-Q water, pH 3.8). From 2 to 12 min the gradient changed to 60% B. The gradient was kept on 60% B for 3 min and followed by a decrease to 10% B. The chromatography was stopped at 25 min. The flow was kept constant at 0.25 mL/min and the column was kept at 25 °C throughout the analysis. The mass spectrometer operated in full scan (range [70.0000–1050.0000]) and positive mode using a spray voltage of 3 kV, capillary temperature of 320 °C, sheath gas at 45, auxiliary gas at 10, and the latter heated to 260 °C. The AGC target was set at 3.0E+006 using a resolution of 70,000. Data collection was performed using the Xcalibur software 4.2.47 (Thermo Scientific, Dilbeek, Belgium). The data analyses were performed by integrating the peak areas (El-Maven–Polly–Elucidata), and cystine was quantified using the known concentration of $^{15}N_2$-cystine spiked in the extraction buffer. Metabolites from glycolysis, the Krebs cycle, amino acids, nucleotides, energy charge, and redox molecules were measured in addition to cystine. The data are depicted as abundancies (log scale) or µM cystine normalized for total protein content. MetaboAnalyst 6.0 software was used to generate volcano plots with a fold change (FC) threshold of 4.0 and *p*-value threshold of 0.05 (two-sample unpaired *t*-test).

2.7. Protein Analysis by PAGE and Western Blot

Cell pellets were homogenized in 1% Sodium Dodecyl Sulfate (SDS, Sigma) together with protease inhibitors (Merck, Hoeilaart, Belgium) and subsequently heated for 5 min at 98 °C. After sonication, the samples were again heated for 5 min at 98 °C. The total protein concentration was determined using the Pierce™ BCA Protein Assay Kit (Thermo Scientific, Dilbeek, Belgium) following the manufacturers' instructions. A total of 10–20 µg of protein was mixed with SDS loading dye (6x) containing β-mercapto-ethanol (10%; VWR, Leuven, Belgium) and subsequently loaded on a 4–15% tris-glycine gel (4–15% Criterion™ TGX™ Precast Midi Protein Gel). The proteins were transferred using a Trans-Blot Turbo Transfer System (Biorad, Temse, Belgium). After transfer, the PVDF membrane was blocked using 5% milk in 0.1% PBS-tritonX-100 solution (215682500; Acros Organics, Geel, Belgium) and subsequently incubated with primary antibodies overnight (ON) at 4 °C (the specification of all antibodies is described in Table S2). Next, the membrane was incubated with a secondary anti-species antibody conjugated with horse radish peroxidase (HRP; Dako Agilent, Leuven, Belgium) in 5% milk in 0.1% PBS-triton solution. The proteins were visualized following incubation with the Clarity™ Western ECL Substrate (Biorad, Temse, Leuven). Images were acquired using the LAS-3000 Imaging system (Fuji, Zaventem, Belgium) or Amersham ImageQuant 800 Fluor (GE Healthcare, Diegem, Belgium) and subsequently quantified with ImageQuant™ TL software V8.2.

To remove N-linked oligosaccharides from glycoproteins, PNGase F treatment (New England Biolabs; Leiden, The Netherlands) was performed following the manufacturers' instructions. Subsequently, samples were processed as indicated before.

2.8. Immunocytochemistry Staining

ciPTECs were seeded in non-detachable chambers (Ibidi, Beloeil, Belgium) and, after 72 h, fixed with 4% paraformaldehyde (PFA; Sigma, Overijse, Belgium) for 20 min at RT. To permeabilize, the ciPTECs were incubated with 0.1% triton X-100 (Acros Organics, Geel, Belgium) for 30 min. The cells were washed with PBS and subsequently blocked for 30 min with 1% bovine serum albumin (BSA; Sigma). After washing with PBS, the cells were incubated ON at 4 °C with primary antibodies diluted in PBS with 0.1% BSA. The next day, the cells were washed with PBS and incubated for 30 min with secondary antibodies (Thermo Scientific, Dilbeek, Belgium) diluted in PBS with 0.1% BSA and DAPI (1/2000, Sigma) diluted in Mowiol mounting medium (Sigma, Overijse, Belgium).

The samples were visualized with a laser scanning confocal microscope (Zeiss LSM 780, Cell Imaging Core (KU Leuven)) in combination with a Plan-Apochromat 63x/1.4 Oil DIC M27 objective (Zeiss, Brussel, Belgium), and the following lasers: 488 nm, 561 nm, 633 nm, and 405 nm (DAPI).

2.9. AlphaMissense Pathogenicity and CADD Scores

We used AlphaMissense via the web resource https://alphamissense.hegelab.org (accessed on 24 January 2024), providing us with the pathogenicity scores and PDBe-mol structure viewer containing the predicted structure of CTNS from AlphaFold using CTNS in the search interface: CTNS_HUMAN, O60931, ENST00000046640.7 [29,40]. We confirmed the subset of mutations in AlphaMissense, which uses pathogenicity scores and classifies it as either likely benign, likely pathogenic, or uncertain based on the structural context of variants (AlphaFold), their evolutionary conservation, and protein language modelling (Table 1) [29,40,41]. The AlphaMissense pathogenicity score of the variants is given as the log-likelihood difference of a residue relative to the reference residue at that position. The Combined Annotation Dependent Depletion (CADD) algorithm measures the deleteriousness of genetic variants. Pre-computed CADD scores for the respective CTNS missense mutants were retrieved from the PopViz webserver (https://hgidsoft.rockefeller.edu/PopViz/, accessed on 24 January 2024) [42].

Table 1. Overview of studied CTNS mutations.

gDNA Mutation	Exon	Protein Mutation	Location	Phenotype	Cystine Transport Activity (%) [A]	AlphaMissense Score [B]	CADD Score [C]	References
c.198_218del21	Exon 5	ITILELP-Del.67–73	N-terminal tail	Juvenile	19 ± 6.1	NA	NA	[24,43–49]
c.544T > C	Exon 8	W182R	2nd TM	Infantile	34 ± 5	0.7778	26.9	[24,43]
c.839A > G	Exon 10	K280R	5th inter-TM loop	Juvenile	0.68 ± 0.9	0.6602	35	[15,24,27,28,50–52]
c.864C > A	Exon 11	N288K	5th inter-TM loop	Infantile	1.6 ± 1.2	0.9942	25	[24,27,45,52,53]
c.893G > A	Exon 11	S298N	5th inter-TM loop	Infantile	77 ± 21	0.5957	29.8	[24,43]
c.969C > G	Exon 11	N323K	6th inter-TM loop	Juvenile	0.14 ± 0.8	0.7791	22.6	[24,45,50,52,54,55]
c.1354G > A	Exon 12	G339R	7th TM	Infantile	−0.8 ± 3.3	0.9803	31	[24,43,56–63]

[A] Cystine transport activity is expressed as mean percentage of WT CTNS activity ± SEM as determined by Kalatzis et al., 2004 [24]. [B] AlphaMissense pathogenicity core: likely benign, 0–0.34; ambiguous, 0.34–0.56; likely pathogenic, 0.564–1.0. [C] CADD scores: less likely pathogenic, 1–10; moderate potential to be pathogenic, 10–20; likely pathogenic, 20–99. NA, non-applicable.

2.10. Statistical Analysis

Data are expressed as the mean ± standard deviation with individual data points shown in each group (replicates of multiple independent experiments). GraphPad 8.0.2 was used to plot all graphs and perform statistical analysis.

3. Results

3.1. Description of the Selected CTNS Mutations

Until now, most in vitro models have studied infantile cystinosis in the context of the 57-kb deletion, resulting in complete loss of the CTNS protein. However, a subset of patients suffers from cystinosis and carry amino acid substitutions [20]. In a recent cohort study, it was shown that 23% of the patients were heterozygous for 57-kb deletion, and 45% had other pathogenic mutations in the *CTNS* gene [23]. In this study, we set out to determine the impact of *CTNS* missense mutations and a small deletion on CTNS transport activity in a clinically relevant kidney-derived proximal tubule epithelial cell model. We selected a subset of CTNS mutations that were located over the whole CTNS protein, and correlated with either infantile or juvenile phenotypes in cystinosis patients: Del.67–73, W182R, K280R, N288K, S298N, and N323K (Figure 1). These mutants were selected because of the discrepancy between the clinical phenotype and the in vitro cystine transport activity reported by Kalatzis et al. [24]. We collected all published information for these mutants in Table 1. Additionally, we determined AlphaMissense pathogenicity and CADD scores for the respective CTNS missense mutants [20,24,29]. W182R, K280R, N288K, S298N, and N323K are predicted to be likely_pathogenic with an AlphaMissense pathogenicity score between 0.5957–0.9942, and CADD scores ranging between 22.6–35.

3.2. Both CTNS^{WT} and CTNS^{mutants} Restore Cystine Content in Cystinosis Cell Models upon Overexpression

For each of the selected mutants, HIV-based lentiviral vectors (LV) were constructed, driving the expression of the respective *CTNS*^{mutant} cDNAs including a C-terminal triple hemagglutinin tag (3HA) from the ubiquitous human *EF1a* promoter (LV_pEF1a-CTNS^{mutant}; Figure 2A). *CTNS* CRISPR-ed (CTNS depleted) conditionally immortalized human proximal tubule epithelial cells (referred to as *CTNS*$^{-/-}$ ciPTECs) were transduced with the respective LVs at low multiplicity of infection (MOI) to ensure single integrated copies, and selected [32]. As a reference, wild-type (WT) *CTNS* cDNA was taken along (LV_pEF1a-CTNS^{WT}). To control for the transduction of CTNS, first a stable cytosolic eGFP overexpression cell line was taken along (LV_ctrl). *CTNS* mRNA levels in CTNS^{WT}- and CTNS^{mutant}-transduced *CTNS*$^{-/-}$ ciPTECs were >2 logs higher compared to the endogenous *CTNS* expression levels in reference *CTNS*$^{+/+}$ ciPTECs (Figure 2B). Furthermore, the protein levels were examined by Western blot analysis (Figure 2C). Because of the heavily glycosylated N-terminus, CTNS^{WT} and the respective CTNS^{mutants} were observed as a diffuse band at ~70 kDa [45]. Removal of the N-linked oligosaccharides by PNGase F treatment shifted the respective proteins to ~41 kDa. For the deletion mutant, CTNS$^{del.67\text{-}73}$, PNGaseF treatment did not affect the migration in the Western analysis, in line with previous reports [45]. Next to normal protein expression, all missense CTNS mutants were located on the lysosomes, as shown by the subcellular co-localisation of CTNS^{WT} and CTNS^{mutants} with lysosomal-associated membrane protein 1 (LAMP1/LA1) (Figure 2D). After validation of protein expression and correct subcellular localisation following stable expression of CTNS^{WT} and CTNS^{mutants}, we performed metabolomic analysis and evaluated the cystine levels. First, we evaluated parental *CTNS*$^{+/+}$ and the CRISPRed *CTNS*$^{-/-}$ cells. Here, no significant alterations were detected in metabolites from glycolysis, the Krebs cycle, energy charges, amino acids, or nucleotides except for cystine, cysteine, and GSSG (Figures 2E and S1A; $p < 0.05$, unpaired t-test). CTNS^{WT} and CTNS^{mutant} addition resulted in a significant reduction in the cystine levels compared to transduction control (compared to LV_ctrl; $p < 0.0001$, one-way Anova, Sidak's multiple comparison test), resulting in cystine levels like parental non-cystinosis cells (*CTNS*$^{+/+}$) (Figure 2E). Additionally, the elevated cysteine and GSSG/(GSH + GSSG) ratio in *CTNS*$^{-/-}$ ciPTECs, known to be altered in cystinosis, showed normalization upon overexpression of any of the CTNS^{mutant} proteins (Figure S1B,C) [64]. Similarly, all CTNS^{mutants}-complemented cystinosis patient-derived fibroblasts showed restored cystine accumulation to CTNS^{WT} levels (Figure S2; compared to LV_ctrl; $p < 0.0001$, one-way Anova, Sidak's multiple comparison test). Taken together, we showed that CTNS^{mutant} proteins expressed well and located to the lysosome as CTNS^{WT}. Moreover, cystine measurements illustrated that a stable introduction of the CTNS^{mutant} proteins in *CTNS*$^{-/-}$ ciPTECs and patient-derived fibroblasts allowed cystine accumulation to revert to levels observed in CTNS^{WT}-complemented ciPTECs and fibroblasts.

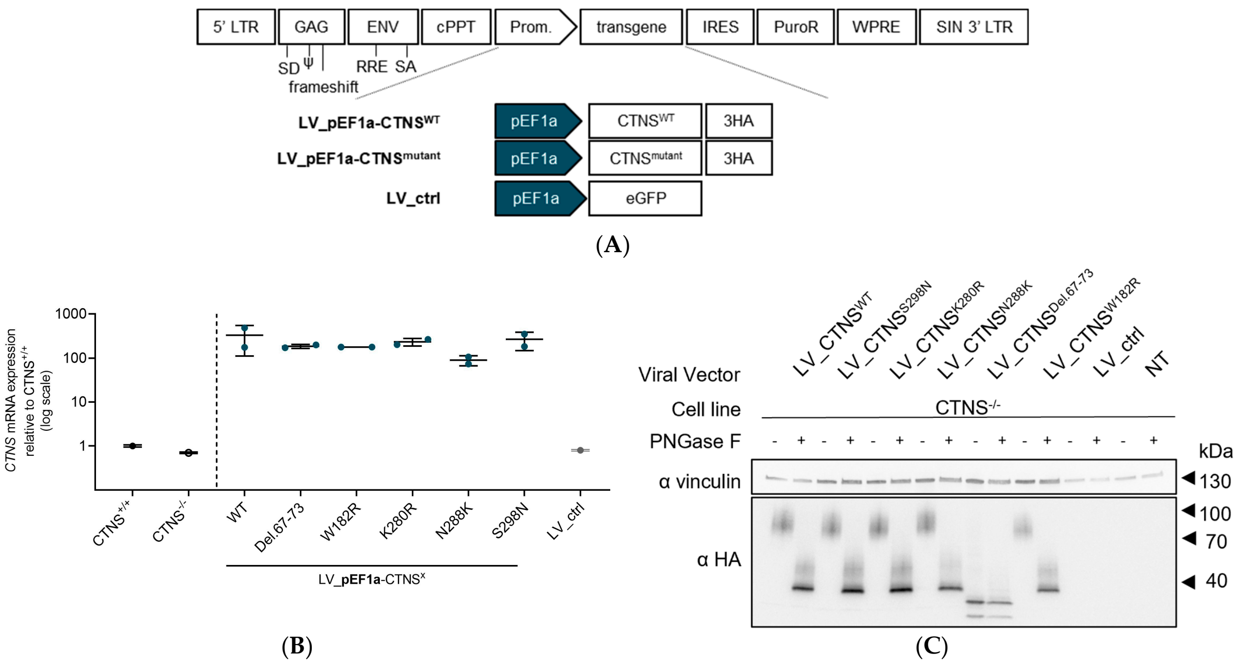

Figure 2. *Cont.*

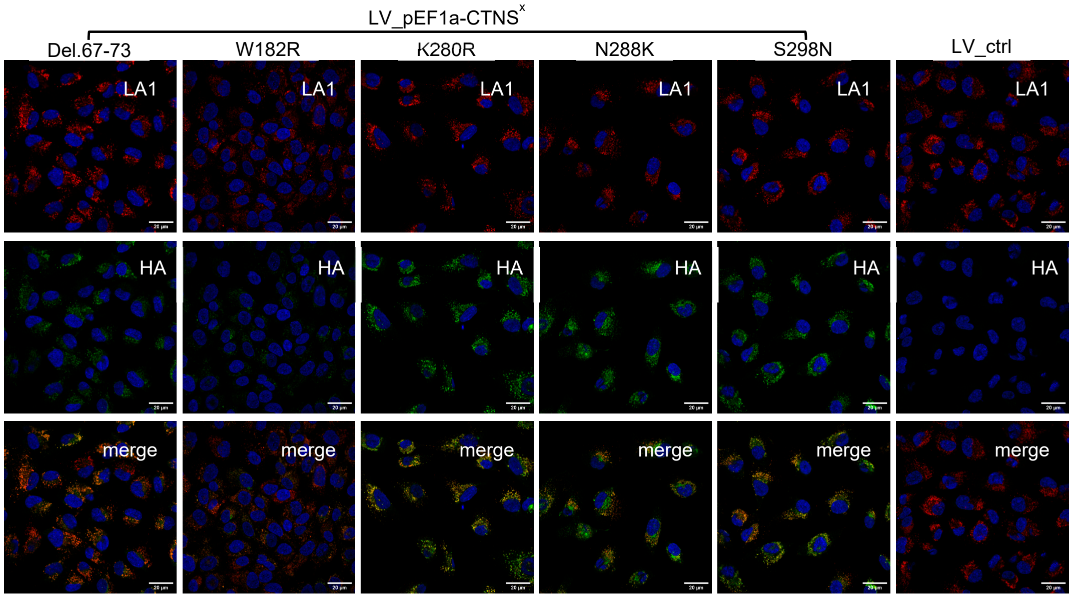

(**D**)

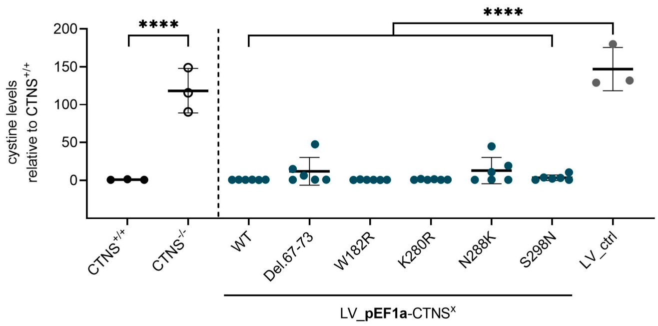

(**E**)

Figure 2. *CTNS^WT* and *CTNS^mutant* cDNA addition after lentiviral vector transduction in CRISPRed *CTNS*$^{-/-}$ ciPTECs greatly reduces the intracellular cystine levels. (**A**) Schematic representation of the lentiviral transfer plasmid setup encoding CTNS$^{\mathrm{WT}}$, CTNS$^{\mathrm{mutant}}$, or eGFP cDNA used to produce the respective lentiviral vectors. *CTNS*$^{-/-}$ ciPTECs were transduced with lentiviral vectors expression of CTNS$^{\mathrm{mutant}}$-3HA and selected using puromycin to obtain ciPTECs expressing at least 1 integrated copy of the transgene construct. (**B**) *CTNS* mRNA expression level analysis (RT-qPCR) on *CTNS*$^{-/-}$ ciPTECs transduced with lentiviral vectors LV_pEF1a-CTNS$^{\mathrm{WT}}$, LV_pEF1a-CTNS$^{\mathrm{mutant}}$, or LV_ctrl. The data are normalized for total mRNA levels of γ-Actin and are presented as the mean ± SD (n = 2). (**C**) Western blot analysis of CTNS-3HA protein expression in *CTNS*$^{-/-}$ ciPTECs transduced with lentiviral vectors LV_pEF1a-CTNS$^{\mathrm{WT}}$, LV_pEF1a-CTNS$^{\mathrm{mutant}}$, or LV_ctrl. Samples were treated with or without PNGase to remove N-glycosylations and normalized for total proteins of vinculin. (**D**) Confocal microscopy images of the immunofluorescence signal of CTNS-3HA (HA, green pseudocolour signal, 633 nm laser) and LAMP1 (LA1, red pseudocolour signal, 561 nm laser) in *CTNS*$^{-/-}$ ciPTECs transduced with either LV_pEF1a-CTNS$^{\mathrm{WT}}$, LV_pEF1a-CTNS$^{\mathrm{mutant}}$, or LV_ctrl. Nuclei were stained with DAPI. Scale bars are 20 µM. (**E**) Cystine measurement (mass spectrometry) of *CTNS*$^{-/-}$ ciPTECs transduced with either LV_pEF1a-CTNS$^{\mathrm{WT}}$, LV_pEF1a-CTNS$^{\mathrm{mutant}}$, or LV_ctrl. The data are presented as the mean ± SD (n = 3 or 6 independent metabolite extracts). Statistical testing was performed with a one-way Anova, Sidak's multiple comparison test. LTR, long terminal repeats; SD, splice donor site; RRE, rev-responsive element; SA, splice acceptor site; cPPT, central polypurine tract; IRES, internal ribosomal entry site; WPRE, woodchuck hepatitis virus posttranscriptional regulatory element; SIN, self-inactivating; LV, lentiviral vector; p, promoter; WT, wild-type; LV_ctrl, LV_pEF1a-eGFP; NT, non-transduced; ****, $p < 0.0001$.

3.3. Physiologically More Relevant $CTNS^{WT}$ Expression Levels Rescue Cystine Accumulation

We hypothesized that the rescue of cystine accumulation in the abovementioned cell models could be explained by the supraphysiological expression levels of $CTNS^{mutant}$ mRNA and $\mathrm{CTNS}^{\mathrm{mutant}}$ protein. To explore more physiological expression levels, we complemented $CTNS^{-/-}$ ciPTECs with $CTNS^{WT}$ cDNA carrying a less potent *EFS* promoter (EF1a-short; p*EFS*) and the *CTNS* promoter (p*CTNS*) to drive transcription, and examined cystine accumulation (Figure 3A) [35,36]. *CTNS* and *EFS* promoter functionality in ciPTECs was confirmed by eGFP expression analysis for LV_eGFP control constructs (LV_pCTNS-eGFP, LV_pEFS-eGFP), demonstrating a 7- and 1.3-fold lower MFI (based on one integrated copy; ~30% eGFP^{+} cells) compared to p*EF1a*-driven expression (Figure S3A). Instead of using eGFP, we from here on, employed control expression constructs of a dead ATP13A2 protein (dATP13A2), a lysosomal transmembrane protein [65]. Next, we assessed $CTNS^{-/-}$ ciPTEC transduced with the respective promoter–$\mathrm{CTNS}^{\mathrm{WT}}$ constructs. Integration of the transgene construct was confirmed by measuring integrated copies (Figure S3B). Expression levels of $CTNS^{WT}$ driven by the *EF1a* promoter resulted in a 160-fold higher expression than endogenous expression in $CTNS^{+/+}$, while the *EFS* and *CTNS* promoter showed 26- and 18-fold higher expression levels, respectively (Figure 3B). $\mathrm{CTNS}^{\mathrm{WT}}$-3HA protein expression was shown by Western blot analysis (Figure 3C). Quantification of the Western blot signals showed a 4- and 33-fold lower protein expression compared to *EF1a*-driven expression, when $CTNS^{WT}$*-3HA* is driven by the *EFS* or *CTNS* promoter, respectively (Figure S3C). For all three promoters, we confirmed lysosomal $\mathrm{CTNS}^{\mathrm{WT}}$ expression by immunocytochemistry staining (Figure S3D). Next, we performed a mass spectrometry analysis to assess the levels of cystine accumulation and demonstrated that cystine levels decreased to $CTNS^{+/+}$ (and LV_pEF1a-$\mathrm{CTNS}^{\mathrm{WT}}$) levels in $CTNS^{-/-}$ ciPTECs after $CTNS^{WT}$ cDNA addition driven by the *EFS* and *CTNS* promoter compared to transduction control (Figure 3D; compared to LV_ctrl; $p < 0.0001$, one-way Anova, Sidak's multiple comparison test). Additionally, the cysteine levels and redox state normalized to parental non-cystinosis $CTNS^{+/+}$ levels, confirming that lower and physiologically more relevant CTNS expression levels were sufficient to reverse the cystinosis phenotype (Figure S3E,F). This prompted us to further evaluate the effect of $\mathrm{CTNS}^{\mathrm{mutants}}$ at lower expression levels.

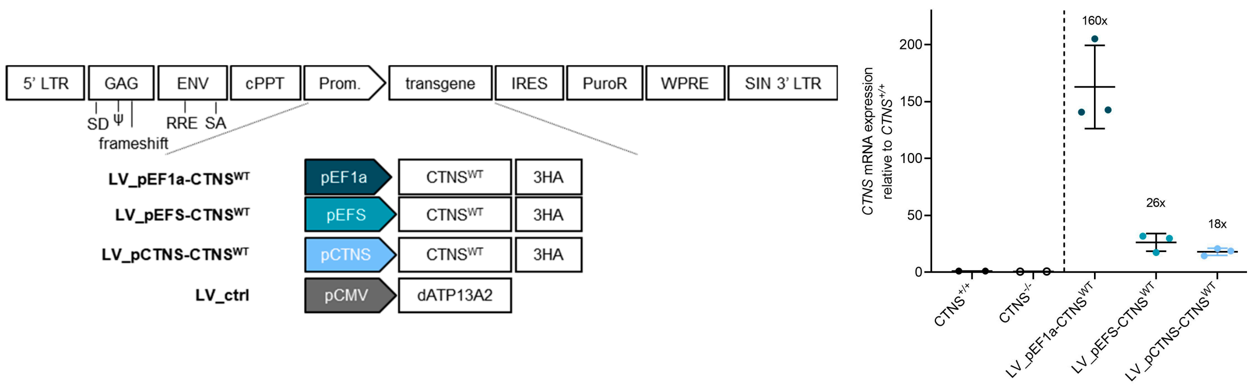

(**A**) (**B**)

Figure 3. *Cont.*

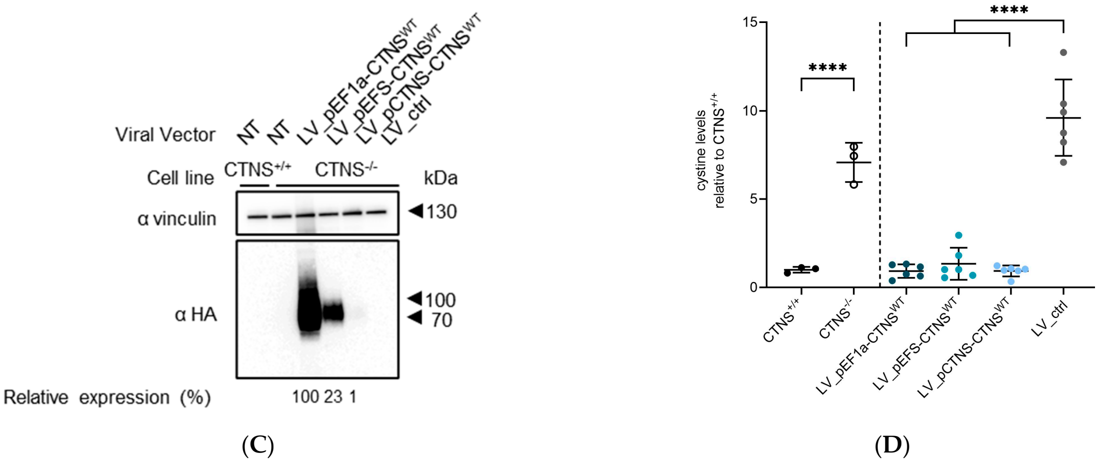

Figure 3. Rescue of the cystinosis phenotype by lower CTNS^{WT} expression enabled by the less potent EFS and CTNS promoters. (**A**) Schematic representation of the lentiviral transfer plasmid setup encoding CTNS^{WT} cDNA driven by either the *EF1a*, *EFS*, or *CTNS* promoter or dATP13A2 cDNA driven by the *CMV* promoter used to produce the respective lentiviral vectors, indicated below. *CTNS*$^{-/-}$ ciPTECs were transduced with lentiviral vectors expression of CTNS^{WT}-3HA and selected using puromycin to obtain ciPTECs expressing at least 1 integrated copy of the transgene construct. (**B**) *CTNS* mRNA expression level analysis (RT-qPCR) in *CTNS*$^{-/-}$ ciPTECs transduced with lentiviral vectors LV_pEF1a-CTNS^{WT}, LV_pEFS-CTNS^{WT}, and LV_pCTNS-CTNS^{WT}. The data are normalized for total mRNA levels of γ-Actin and are presented as the mean ± SD (n = 3). (**C**) Western blot analysis of CTNS^{WT}-3HA protein expression in *CTNS*$^{-/-}$ ciPTECs transduced with lentiviral vectors LV_pEF1a-CTNS^{WT}, LV_pEFS-CTNS^{WT}, LV_pCTNS-CTNS^{WT}, or LV_ctrl. Samples normalized for total proteins of vinculin. (**D**) Cystine measurement (mass spectrometry) of *CTNS*$^{-/-}$ ciPTECs transduced with either LV_pEF1a-CTNS^{WT}, LV_pEFS-CTNS^{WT}, LV_pCTNS-CTNS^{WT}, or LV_ctrl. The data are presented as the mean ± SD (n = 3 or 6 independent metabolite extracts). Cystine (Abundance) was normalized to protein content (µg/µL). Statistical testing was performed with a one-way Anova, Sidak's multiple comparison test. LV, lentiviral vector; p, promoter; WT, wild-type; LV_ctrl, LV_pCMV-dATP13A2; NT, non-transduced; ****, $p < 0.0001$.

3.4. *CTNS^{mutant} Expression Driven by EFS- and CTNS Promoter Still Reverts Cystine Levels*

We transduced *CTNS*$^{-/-}$ ciPTECs with LV vectors encompassing *CTNS^{mutants}* cDNA driven by the *EFS* or the *CTNS* promoter. Integration of the transgene construct was confirmed by measuring integrated copies (Figure S4A). For both promoters, CTNS^{mutant} protein expression was confirmed by Western blot analysis, showing substantially lower proteins levels for *CTNS* promoter-driven constructs (with some of the CTNS^{mutants} barely detectable), as expected with CTNS$^{del67\text{-}73}$ and CTNS^{W182R} showing lower protein levels in both conditions (Figure 4B). The enhanced contrast blot shows CTNS$^{del67\text{-}73}$ at 25 kDa and visualizes the low expression levels of *CTNS* promoter-driven constructs (Figure S4B). Scanning of the Western blot signals showed on average a 14-fold lower protein expression level when *CTNS^{mutants}* cDNA was driven by the *CTNS* promoter (Figure S4C). Still, these physiologically more relevant expression levels of CTNS^{mutants} reduced the cystine content in *CTNS*$^{-/-}$ ciPTECs significantly compared to the transduction control ($p < 0.0001$ compared to LV_ctrl, one-way Anova, Sidak's multiple comparison test), reaching *CTNS*$^{+/+}$ levels for most of the conditions, even though the protein levels of CTNS^{mutants} were substantially lower for the *CTNS* promoter-driven constructs (Figure 4C). Interestingly, two conditions, p*CTNS*-CTNS$^{del67\text{-}73}$ and p*CTNS*-CTNS^{N288K}, resulted in a significant drop in cystine accumulation compared to the transduction control ($p < 0.0001$, one-way Anova, Sidak's multiple comparison test), but were still significantly higher than pCTNS-CTNS^{WT} ($p < 0.0001$ compared to LV_CTNS^{WT}, one-way Anova, Sidak's multiple comparison test). Even though the results obtained were exciting, the fact that cystine accumulation in most cases was completely rescued in our cell model, even when using expression levels that are close to physiological levels, prompted us to demonstrate that this is not the case for every single *CTNS* missense mutation. Therefore, we additionally selected another missense CTNS mutation, G339R, that is associated with the infantile form of cystinosis, and is predicted to be pathogenic based on the AlphaMissense pathogenicity score and the CADD score (0.9803 and 29, respectively; Table 1). We complemented $CTNS^{-/-}$ ciPTECs with LV-encoding $CTNS^{G339R}$ cDNA driven by the *EFS* promoter and selected the transduced cells. Integration of the $CTNS^{G339R}$ transgene construct was confirmed by measuring integrated copies (Figure S5A). $CTNS^{WT}$ and $CTNS^{K280R}$ were taken along as controls. Protein expression was corroborated by Western blot analysis and immunohistochemistry, demonstrating that $CTNS^{G339R}$, in line with the other CTNS point mutations assessed, expressed well and localised to the lysosomes (Figure 5A,B). Contrary to $CTNS^{WT}$ and $CTNS^{K280R}$, $CTNS^{G339R}$ did not restore the cystine accumulation, underscoring that not all *CTNS* missense mutations behave the same (Figure 5C). Similarly, cysteine accumulation was also not restored (Figure S5B).

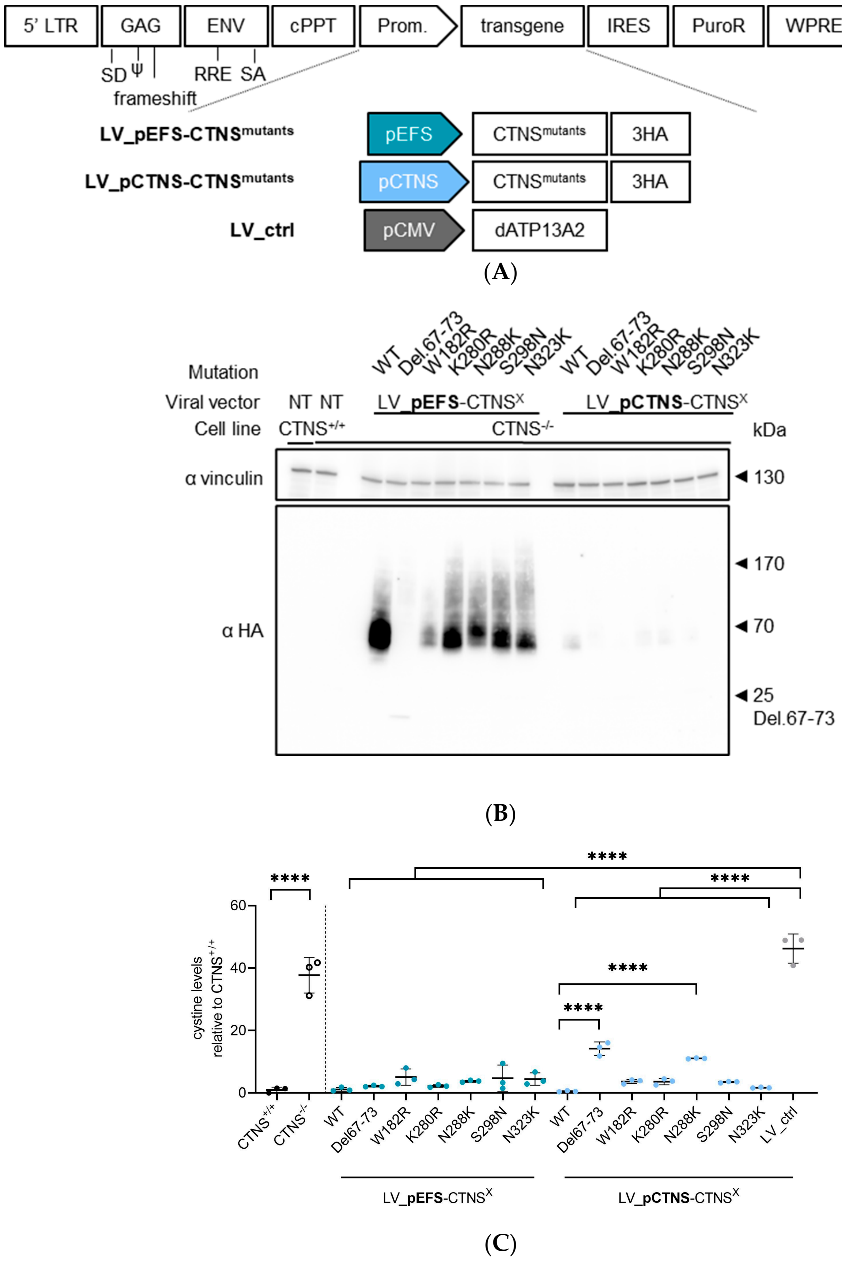

Figure 4. Different promoters exhibit rescue of mutants even with low activity. (**A**) Schematic representation of the lentiviral transfer plasmid setup encoding $CTNS^{mutants}$ cDNA driven by either

the *EF1a*, *EFS*, or *CTNS* promoter or dATP13A2 cDNA driven by the *CMV* promoter used to produce the respective lentiviral vectors, indicated below. *CTNS*$^{-/-}$ ciPTECs were transduced with lentiviral vectors expression of CTNS$^{\mathrm{WT}}$-3HA or CTNS$^{\mathrm{mutant}}$-3HA and selected using puromycin to obtain a ciPTECs expressing at least 1 integrated copy of the transgene construct. (**B**) Western blot analysis of CTNS$^{\mathrm{WT\ or\ mutant}}$-3HA protein expression in *CTNS*$^{-/-}$ ciPTECs transduced with lentiviral vectors LV_pEFS-CTNS$^{\mathrm{WT\ or\ mutant}}$, LV_pCTNS-CTNS$^{\mathrm{WT\ or\ mutant}}$, or LV_ctrl. Samples normalized for total proteins of vinculin. (**C**) Cystine measurement (mass spectrometry) of *CTNS*$^{-/-}$ ciPTECs transduced with lentivectors LV_pEFS-CTNS$^{\mathrm{WT\ or\ mutant}}$, LV_pCTNS-CTNS$^{\mathrm{WT\ or\ mutant}}$, or LV_ctrl. The data are presented as the mean ± SD (n = 3 independent metabolite extracts). Statistical testing was performed with a one-way Anova, Sidak's multiple comparison test. LV, lentiviral vector; p, promoter; WT, wild-type; LV_ctrl, LV_pCMV-dATP13A2; NT, non-transduced; ****, $p < 0.0001$.

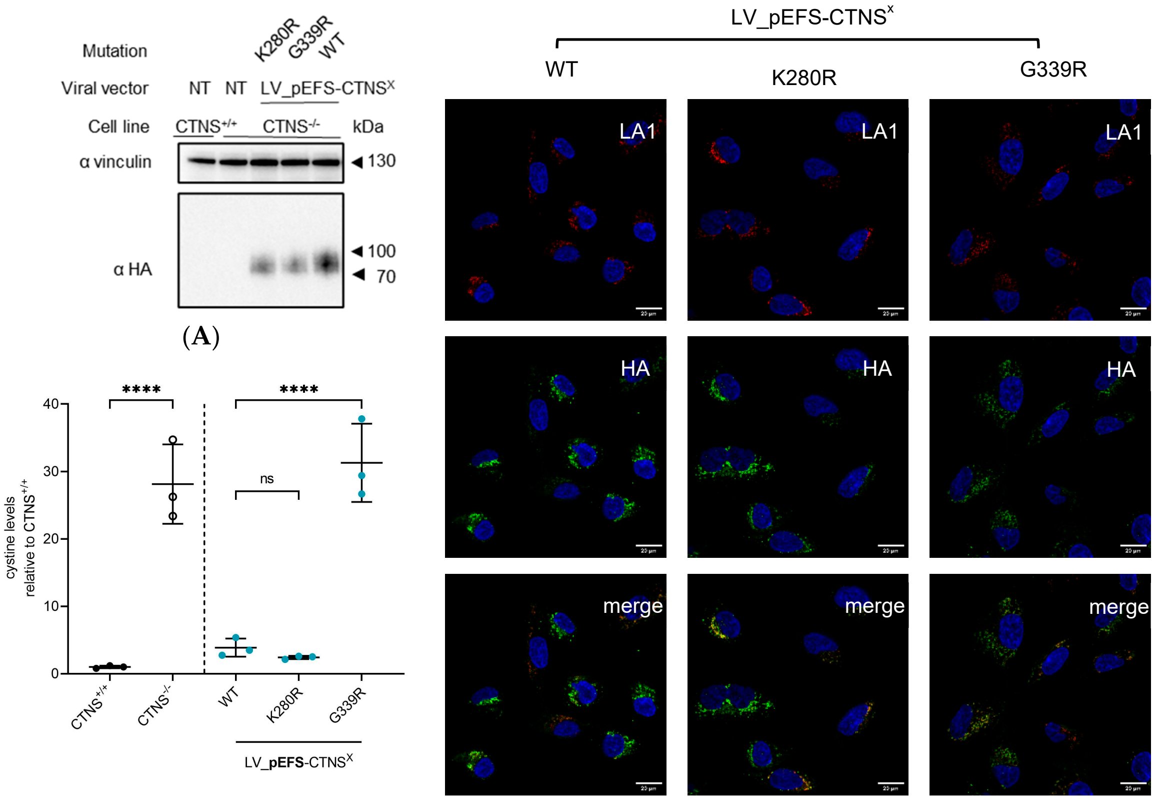

Figure 5. G339R mutant overexpression shows no rescue in cystine accumulation upon cDNA addition in *CTNS*$^{-/-}$ ciPTECs. (**A**) Western blot analysis of CTNS$^{\mathrm{X}}$-3HA protein expression in *CTNS*$^{-/-}$ ciPTECs transduced with lentiviral vectors LV_pEFS-CTNS$^{\mathrm{WT}}$ or pEFS-CTNS$^{\mathrm{K280R\ or\ G339R}}$. Samples normalized for total proteins of vinculin. (**B**) Confocal microscopy images of the immunofluorescence signal of CTNS$^{\mathrm{X}}$-3HA and LAMP1 in *CTNS*$^{-/-}$ ciPTECs transduced with either LV_pEFS-CTNS$^{\mathrm{WT}}$ or LV_pEFS-CTNS$^{\mathrm{K280R\ or\ G339R}}$. Nuclei were stained with DAPI. Scale bars are 20 µM. (**C**) Cystine measurement (mass spectrometry) of *CTNS*$^{-/-}$ ciPTECs transduced with lentiviral vectors LV_pEFS-CTNS$^{\mathrm{WT}}$ or pEFS-CTNS$^{\mathrm{K280R\ or\ G339R}}$. The data are presented as the mean ± SD (n = 3 independent metabolite extracts). Statistical testing was performed with a one-way Anova, Sidak's multiple comparison test. LV, lentiviral vector; p, promoter; WT, wild-type; NT, non-transduced; ****, $p < 0.0001$; ns, nonsignificant.

4. Discussion

Hitherto, the study of cystinosis has largely focused on the most common Caucasian mutation resulting in complete loss of the CTNS protein due to a 57 kb deletion [14,21,22]. Still, close to 50% of patients living with cystinosis carry point mutations and smaller indels in the CTNS protein and the effect of these mutations on the protein and its function is only poorly studied. We used a clinically relevant CTNS-depleted kidney cell model and patient-derived *CTNS*$^{-/-}$ fibroblasts to stably express specific CTNS mutants from different promoters (Table 1) [32]. The mutations selected were associated with infantile and juvenile nephropathic cystinosis and were selected based on the discrepancies between in vitro cystine transport activity observed by Kalatzis et al. and the clinical phenotype [24]. Their pathogenicity scores based on AlphaMissense and CADD score indicated that all mutations tested were likely to be pathogenic, in line with the phenotype of the patients carrying the mutation (Table 1). When introducing the *CTNS*^{mutants} driven by the *EF1a* promoter in CTNS-depleted cells (patient-derived fibroblasts or CRISPRed *CTNS*$^{-/-}$ PTECs) using LVs, all proteins expressed well, located to the lysosome, and normalized cystine to WT levels (*CTNS*$^{+/+}$) (Figure 2D). *EFS* promoter- and *CTNS* promoter-driven CTNS^{WT} protein expression levels were significantly lower compared to the *EF1a* promoter-driven constructs (4- to 33-fold, respectively, Figure 3B,C) and rescued cystine accumulation. Still, the mRNA expression levels were 18–26-fold higher than the endogenous *CTNS* mRNA in *CTNS*$^{+/+}$ ciPTECs, suggesting that the endogenous *CTNS* promoter together with additional regulatory elements limits expression [35,66]. A possible explanation may be the fact that our constructs only include the open reading frame of *CTNS*, lacking the UTR and intronic sequences, which may contribute to the higher mRNA levels. Moreover, the LV constructs encompass an RNA stabilizing WPRE sequence, and the integrated lentiviral vector copy number, which also contribute to the overall higher *CTNS* expression levels [67]. We detected more integrated copies when CTNS^{mutants} and the puromycin selection cassette was driven by the weaker *CTNS* promoter, resulting in higher expression levels (Figure S4B). Intriguingly, also when using the less potent *EFS* and *CTNS* promoters, all CTNS^{mutants} restored the cystine accumulation to WT levels when introduced in *CTNS*$^{-/-}$ ciPTECs, suggesting that this subset of CTNS^{mutants} were still functional, even at near physiological expression levels. CTNS$^{del.67\text{-}73}$ and CTNS^{N288K} showed significant but incomplete rescue of cystine accumulation, in contrast with the other mutants when driven by the *CTNS* promoter (Figure 4C). Both were reported to degrade faster compared to CTNS^{WT} [45,49]. In addition, CTNS$^{Del.67\text{-}73}$ was shown to be unable to exit the ER. CTNS^{N288K} is located at the 5th inter-transmembrane loop, which contains the PQ-motif, important for H^+ and cystine co-transport and was shown to abolish the interaction with V-ATPase-regulator-rag complex [52,68]. In a recent paper by Guo et al. on CTNS protein structure, CTNS^{N288K} was shown to induce structural changes in CTNS favouring a cytosol-open conformation [27]. In addition, CTNS^{K280} was shown to be an important AA in the cystine binding pocket [27,28]. In our study, we showed that CTNS^{K280R} still restored transport activity. As lysine and arginine both have positively charged side chains, this suggests that this mutation has little effect on the binding site, which is consistent with the observation of a juvenile phenotype. The inclusion of CTNS^{G339R} as an additional control validated our model and underscored that not all CTNS^{mutants} rescue cystine accumulation upon stable overexpression: even though the CTNS^{G339R} protein expressed well and located to the lysosomes, in line with other mutants, cystine levels did not lower (Figure 5). We suggest that the substitution of glycine with arginine induces a significant alteration, as it converts a single hydrogen atom into a positively charged side chain. Furthermore, results from a recent study, employing cystinosis mouse PTECs transduced with CTNS^{G339R}-HA driven by the strong *CMV* promoter using an adenoviral vector corroborates our findings, as cystine accumulation remained elevated [69]. Therefore, these comprehensive evaluations collectively highlight the G339R mutation's incapacity to ameliorate cystine accumulation, validating its deleterious effect on CTNS' function. Despite the recent studies published on CTNS' structure, it is worth highlighting that our knowledge on the various domains of CTNS, and how mutations influence the domains and CTNS' function, remains limited [27,28].

The fact that we observed different transport activities than previous studies may be explained by the cell lines employed, together with the overexpression system. Kalatzis and Guo et al. used transient transfection of non-human cells driving *CTNS* cDNA from a potent *CMV* promoter [24,27]. Transient transfection results in acute upregulation of

CTNS mRNA and protein production, whereas we employed stable transduction using LVs aiming at a single integrated copy and using less potent promoters. Additionally, it is conceivable to consider that the massive overexpression and the relocalisation of CTNS to the plasma membrane in the Kalatzis setup may affect functional aspects important for stabilization, CTNS conformation, and/or for the biological function of CTNS. Lastly, our in vitro data underscore that in silico predictive tools like AlphaMissense and CADD scores are interesting, but that functional assays are still required to corroborate these predictions. Discrepancies in AlphaMissense pathogenicity scores, CADD scores, and our in vitro experiments reveal challenges in correlating the effect of $\mathrm{CTNS}^{\mathrm{mutants}}$ on protein structure with the degree of cystine transport. This underscores the limitations in the use of predictive tools for cellular and functional phenotypes, even though these tools are instructive in genome-wide association studies to provide an initial judgement for a newly detected mutation.

Our study encountered notable limitations. First, the lack of reliable antibodies to detect CTNS endogenously presented a significant challenge and made us unable to detect endogenous CTNS at the protein level and difficult to interpret protein-to-mRNA data. This limitation necessitated the use of LVs containing 3HA-tagged *CTNS* cDNA. However, it is important to note that our study opted for stable expression over transient approaches, ensuring protein expression levels as closely as possible resembling endogenous expression levels and a CTNS protein locating to the lysosomal membrane.

In our approach, we used a clinically relevant human cell model ($CTNS^{-/-}$ CRISPRed ciPTECs), enhancing the translational relevance of our findings, and relied on metabolomic analysis to assess cystine accumulation [32]. Our findings indicate that several $\mathrm{CTNS}^{\mathrm{mutants}}$ are functional in our addback model (cystine transport), however it is important to mention that the same mutants in patients still result in disease (infantile and juvenile cystinosis), with poor clinical outcome measures, like for kidney survival. This discrepancy may in part be due to the use of cells in the clinical assay that cycle less and accumulate more cystine, whereas our in vitro cell models proliferate and therefore overall carry lower cystine concentrations. Although these limitations are intrinsic to the current state of the field, our methodology aimed to mitigate potential biases and uphold scientific credibility. Taken together, our study underscores that there is a need for a more nuanced interpretation of *CTNS* mutations, revealing variable cystine transport activity for different *CTNS* mutations, similar to observations in cystic-fibrosis-associated *CFTR* mutations [70]. For example, a subset of mutants may result in folding or trafficking errors that in turn influence protein stability, and result in reduced CTNS protein at the lysosomal membrane. Indeed, a drug shown to improve protein folding (chemical chaperones such as CFTR corrector, Corr4a) was shown to restore 70% of the cystine accumulation in patient-derived fibroblasts carrying $\mathrm{CTNS}^{del.67\text{-}73}$ [49]. Additionally, frameshifts, splicing, or nonsense mutations can result in a premature stop codon leading to little or no CTNS protein expression. Since 15% of patients with cystinosis have nonsense mutations (most common mutation: $\mathrm{CTNS}^{\mathrm{W138X}}$), there is a possibility to apply translational readthrough [43]. Helip-Wooley et al. showed that gentamycin-induced readthrough of exogenous $\mathrm{CTNS}^{\mathrm{W183X}}$-GFP in HEK293Ts and in patient-derived cystinosis fibroblasts heterozygous for W138X led to reduced cystine accumulation [71]. Brasell et al. further showed that geneticin (G418) treatment induced translational readthrough of $\mathrm{CTNS}^{\mathrm{W138X}}$ constructs transfected in HEK293Ts and expression of full length CTNS in homozygous W138X fibroblasts resulting in decreased cystine accumulation [72]. As these compounds are known to cause renal and cochlear toxicity, a modified aminoglycoside without toxicity, called ELX-02, was developed. This aminoglycoside is currently in a phase 2 clinical trial for cystic fibrosis. This novel aminoglycoside produced a functional CTNS protein and reduced cystine accumulation, comparable to cysteamine treatment in cystinosis mice and $\mathrm{CTNS}^{\mathrm{W138X}}$-cultured fibroblasts without displaying cyto- and nephrotoxicity [73]. Identifying and characterizing these mutations will allow us to create a functional classification of CTNS mutants, as was installed for CFTR. In addition, the identification of specific mutation-induced functional effects provides a foundation for the development of precision medicine for cystinosis as is seen for cystic fibrosis, where depending on the class of functional defect, a different therapy is put forward [70].

The complexity surrounding the correlation between the different clinical phenotypes (infantile, juvenile, and ocular) and the mutations affecting *CTNS* is a challenging issue. Since there is considerable variability in patient phenotype, the use of genotype to make statements of prognosis is not recommended. In a recent international cohort study by Emma et al., with genetic data available for 329 individuals, 33% exhibited homozygosity for the common 57-kb deletion, 23% were heterozygous for the same deletion, and 45% had other pathogenic *CTNS* variants [23]. No apparent differences in kidney survival were observed between patients with homozygous or heterozygous 57-kb deletions and those with other pathogenic *CTNS* variants. Similarly, a study by Veys et al. involving 52 patients from 26 pairs of index and sibling patients, found no significant difference in the age at ESKD between those with homozygous 57 kb deletions and those with other pathogenic variants. However, both studies' lack of information on the *CTNS* variants' severity, particularly regarding missense variants, is determined. This underscores the need for more nuanced classification within this category and considering heterozygosity with the 57 kb deletion. An additional layer of complexity is introduced by the various (unknown) functions of CTNS as it is suggested that its role extends beyond mere cystine transport [64]. However, cystine accumulation remains the major hallmark of the disease, and a cornerstone for both diagnosis and treatment. In addition, cystine depletion was shown to be the determining factor, in contrast to the genotype, defining disease outcome (kidney survival) [23]. Most *CTNS* missense mutations have not been functionally characterized, and for most the pathogenic potential remains unclear. To decipher the correlation between *CTNS* mutations and the functional and clinical phenotypes in cystinosis, integrating computational tools with empirical data remains crucial. Moreover, analysing clinical data from well-established cystinosis patient-cohorts focused on specific genotypes is of great interest and is paramount to understand the disease mechanism and to help establish precision medicine. ERKNet and RaDiCo ECYSCO are actively working on a big cohort dataset that includes the patient genotypes and clinical phenotypes for cystinosis [74,75].

In conclusion, we here present an alternative cell model to assess $\mathrm{CTNS}^{\mathrm{mutants}}$ function to better understand discrepancies between genotype, cystine transport function, and clinical phenotype. Our findings indicate that several $\mathrm{CTNS}^{\mathrm{mutants}}$ do possess residual transport activity. It should be further explored whether patients carrying missense mutants having some residual transport activity have a milder cystinosis phenotype than those with mutations completely ablating cystine transport. These results indicate that at least for some mutants pharmacologically, an improvement of protein stability in patient-derived cells may result in (partial) rescue of the cystine accumulation phenotype. Additional in vitro studies to examine the effect of $\mathrm{CTNS}^{\mathrm{mutant}}$ expression on cellular processes are needed to determine the potential of a therapeutic approach and to exclude negative effects.

Supplementary Materials: The following supporting information can be downloaded at: https://www.mdpi.com/article/10.3390/cells13070646/s1. Figure S1: $\mathrm{CTNS}^{\mathrm{WT}}$ and $\mathrm{CTNS}^{\mathrm{mutant}}$ cDNA addition after LV transduction in CRISPRed $CTNS^{-/-}$ ciPTECs reduces the intracellular cysteine and redox levels; Figure S2: $CTNS^{WT}$ and $CTNS^{mutant}$ cDNA addition after LV transduction in cystinosis patient-derived fibroblasts greatly reduces the intracellular cystine levels; Figure S3: Weaker promoters leading to lower $\mathrm{CTNS}^{\mathrm{WT}}$ expression are still able to rescue the cystinosis phenotype; Figure S4: Different promoters showing rescue of mutants even with low activity; Figure S5: G339R mutant overexpression shows no rescue in cystine accumulation upon cDNA addition in $CTNS^{-/-}$ ciPTECs; Table S1: Overview of primer sequences; Table S2: Overview of primary and secondary antibodies.

Author Contributions: Conceptualization, L.M., R.G. and D.D.; methodology, L.M., D.D. and M.S. (Maxime Smits); software, L.M.; validation, L.M. and R.G.; formal analysis, L.M., R.G. and D.D.; investigation, L.M. and R.G.; resources, L.M., R.G. and E.L.; data curation, L.M. and R.G.; writing—original draft preparation, L.M. and R.G.; writing—review and editing, L.M, R.G., D.D., E.L. and M.S. (Maurilio Sampaolesi); visualization, L.M.; supervision, R.G., E.L. and M.S. (Maurilio Sampaolesi);

project administration, R.G.; funding acquisition, R.G. and E.L. All authors have read and agreed to the published version of the manuscript.

Funding: This work was funded by the FWO PhD scholarship of D. David (180936-1S22921N-SW), FWO grant (G056521N) to Rik Gijsbers, and the KU Leuven C1 Grant to Elena Levtchenko and Rik Gijsbers (C14/17/11). We acknowledge Cystinosis Ireland and the Cystinosis Foundation UK co-funded Research Award 2021 (CI-CFUK 2021-02 PI Gijsbers, Sampaolesi, Levtchenko). Elena Levtchenko is a member of the European Reference Kidney Network (ERKNet) and is supported by a European Research Council Consolidator grant 101045467—NEOGRAFT and by Cystinosis Ireland—HRB grant (HRCI-HRB-2022-014). Rik Gijsbers coordinates the GET-IN project that received funding from the European Union's Framework Program for Research and Innovation, EC HORIZON–MSCA-2023-DN Grant Agreement No. 10111988, and is a beneficiary of the ORGESTRA project funded by the EC HORIZON–MSCA-2023-DN-JD (Grant Agreement No 101120108), coordinated by the University of Utrecht.

Institutional Review Board Statement: Not applicable.

Data Availability Statement: All data are available on request to Rik Gijsbers (rik.gijsbers@kuleuven.be).

Acknowledgments: We gratefully acknowledge the R. Masereeuw and M. Janssen (Utrecht University, The Netherlands) for providing the $CTNS^{-/-}$ ciPTEC cell line and K. Veys for his critical reading. We also acknowledge our use of the facilities and equipment of the Leuven Viral Vector Core facility (R. Gijsbers, KU Leuven, Belgium), VIB Metabolomics Core (B. Ghesquière—Sam De Craemer, KU Leuven, Belgium), and Cell and Tissue Imaging Core (P. Vanden Berghe, KU Leuven, Belgium).

Conflicts of Interest: The authors declare no conflicts of interest.

References

1. Jean, G.; Fuchshuber, A.; Town, M.M.; Gribouval, O.; Schneider, J.A.; Broyer, M.; Hoff, W.V.N.T.; Niaudet, P.; Antignac, C. High-Resolution Mapping of the Gene for Cystinosis, Using Combined Biochemical and Linkage Analysis. *Am. J. Hum. Genet.* **1996**, *58*, 535–543. [PubMed]
2. Town, M.; Jean, G.; Cherqui, S.; Attard, M.; Forestier, L.; Whitmore, S.A.; Gallen, D.F.; Gribouval, O.; Broyer, M.; Bates, G.P.; et al. A Novel Gene Encoding an Integral Membrane Protein Is Mutated in Nephropathic Cystinosis. *Nat. Genet.* **1998**, *18*, 319–324. [CrossRef] [PubMed]
3. Piccolo, F.; Roberds, S.L.; Jeanpierre, M.; Leturcq, F.; Azibi, K.; Beldjord, C.; Carrié, A.; Récan, D.; Chaouch, M.; Reghis, A.; et al. Linkage of the Gene for Cystinosis to Markers on the Short Arm of Chromosome 17. *Nat. Genet.* **1995**, *10*, 246–248. [CrossRef]
4. Gahl, W.A.; Tietze, F.; Bashan, N.; Bernardini, I.; Raiford, D.; Schulman, J.D. Characteristics of Cystine Counter-Transport in Normal and Cystinotic Lysosome-Rich Leucocyte Granular Fractions. *Biochem. J.* **1983**, *216*, 393–400. [CrossRef] [PubMed]
5. Kalatzis, V.; Antignac, C.; Gasnier, B.; Cherqui, S.S.; Antignac, C.; Gasnier, B.; Cherqui, Â.; Kalatzis, V.; Antignac, C.; Gasnier, B.; et al. Cystinosin, the Protein Defective in Cystinosis, Is a H+-Driven Lysosomal Cystine Transporter. *EMBO J.* **2001**, *20*, 5940–5949. [CrossRef] [PubMed]
6. Gahl, W.A.; Bashan, N.; Tietze, F.; Bernardini, I.; Schulman, J.D. Cystine Transport Is Defective in Isolated Leukocyte Lysosomes from Patients with Cystinosis. *Science* **1982**, *217*, 1263–1265. [CrossRef] [PubMed]
7. Schulman, J.D.; Bradley, K.H.; Seegmiller, J.E. Cystine: Compartmentalization within Lysosomes in Cystinotic Leukocytes. *Science* **1969**, *166*, 1152–1154. [CrossRef] [PubMed]
8. Schneider, J.A.; Bradley, K.; Seegmiller, J.E. Increased Cystine in Leukocytes from Individuals Homozygous and Heterozygous for Cystinosis. *Science* **1967**, *157*, 1321–1322. [CrossRef] [PubMed]
9. Jonas, A.J.; Greene, A.A.; Smith, M.L.; Schneider, J.A. Cystine Accumulation and Loss in Normal, Heterozygous, and Cystinotic Fibroblasts. *Proc. Natl. Acad. Sci. USA* **1982**, *79*, 4442–4445. [CrossRef] [PubMed]
10. Goldman, H.; Scriver, C.R.; Aaron, K.; Sc, M. Adolescent Cystinosis: Comparisons with Infantile and Adult Forms. *Pediatrics* **1971**, *47*, 979–988. [CrossRef] [PubMed]
11. Nesterova, G.; Gahl, W. Nephropathic Cystinosis: Late Complications of a Multisystemic Disease. *Pediartric Nephrol.* **2008**, *23*, 863–878. [CrossRef] [PubMed]
12. Schneider, J.A.; Wong, V.; Bradley, K.; Seegmiller, J.E. Biochemical Comparisons of the Adult and Childhood Forms of Cystinosis. *N. Engl. J. Med.* **1968**, *279*, 1253–1257. [CrossRef] [PubMed]
13. Wilmer, M.J.; Schoeber, J.P.; Van Den Heuvel, L.P.; Levtchenko, E.N. Cystinosis: Practical Tools for Diagnosis and Treatment. *Pediatr. Nephrol.* **2011**, *26*, 205–215. [CrossRef] [PubMed]
14. Gahl, W.A.; Thoene, J.G.; Schneider, J.A. Medical Progress: Cystinosis. *N. Engl. J. Med.* **2002**, *347*, 111–121. [CrossRef] [PubMed]
15. Servais, A.; Morinière, V.; Grünfeld, J.P.; Noël, L.H.; Goujon, J.M.; Chadefaux-Vekemans, B.; Antignac, C. Late-Onset Nephropathic Cystinosis: Clinical Presentation, Outcome, and Genotyping. *Clin. J. Am. Soc. Nephrol.* **2008**, *3*, 27–35. [CrossRef] [PubMed]

16. Anikster, Y.; Lucero, C.; Guo, J.; Huizing, M.; Shotelersuk, V.; Bernardini, I.; McDowell, G.; Iwata, F.; Kaiser-Kupfer, M.I.; Jaffe, R.; et al. Ocular Nonnephropathic Cystinosis: Clinical, Biochemical, and Molecular Correlations. *Pediatr. Res.* **2000**, *47*, 17–23. [CrossRef] [PubMed]
17. Brodin-sartorius, A.; Tête, M.-J.J.; Niaudet, P.; Antignac, C.; Guest, G.; Ottolenghi, C.; Charbit, M.; Moyse, D.; Legendre, C.; Lesavre, P.; et al. Cysteamine Therapy Delays the Progression of Nephropathic Cystinosis in Late Adolescents and Adults. *Kidney Int.* **2012**, *81*, 179–189. [CrossRef] [PubMed]
18. Emma, F.; Nesterova, G.; Langman, C.; Labbé, A.; Cherqui, S.; Goodyer, P.; Janssen, M.C.; Greco, M.; Topaloglu, R.; Elenberg, E.; et al. Full Review Nephropathic Cystinosis: An International Consensus Document. *Nephrol. Dial. Transplant.* **2014**, *29*, 87–94. [CrossRef] [PubMed]
19. HGMD®Gene Result. Available online: https://www.hgmd.cf.ac.uk/ac/gene.php?gene=CTNS (accessed on 4 October 2023).
20. David, D.; Berlingerio, P.; Elmonem, A.; Princiero Berlingerio, S.; Elmonem, M.A.; Oliveira Arcolino, F.; Soliman, N.; Van Den Heuvel, B.; Gijsbers, R.; Levtchenko, E.; et al. Molecular Basis of Cystinosis: Geographic Distribution, Functional Consequences of Mutations in the CTNS Gene, and Potential for Repair. *Nephron* **2019**, *141*, 133–146. [CrossRef]
21. Touchman, J.W.; Anikster, Y.; Dietrich, N.L.; Braden Maduro, V.V.; McDowell, G.; Shotelersuk, V.; Bouffard, G.G.; Beckstrom-Sternberg, S.M.; Gahl, W.A.; Green, E.D. The Genomic Region Encompassing the Nephropathic Cystinosis Gene (CTNS): Complete Sequencing of a 200-Kb Segment and Discovery of a Novel Gene within the Common Cystinosis-Causing Deletion. *Genome Res.* **2000**, *10*, 165–173. [CrossRef]
22. Anikster, Y.; Lucero, C.; Touchman, J.W.; Huizing, M.; McDowell, G.; Shotelersuk, V.; Green, E.D.; Gahl, W.A. Identification and Detection of the Common 65-Kb Deletion Breakpoint in the Nephropathic Cystinosis Gene (CTNS). *Mol. Genet. Metab.* **1999**, *66*, 111–116. [CrossRef] [PubMed]
23. Emma, F.; van't Hoff, W.; Hohenfellner, K.; Topaloglu, R.; Greco, M.; Ariceta, G.; Bettini, C.; Bockenhauer, D.; Veys, K.; Pape, L.; et al. An International Cohort Study Spanning Five Decades Assessed Outcomes of Nephropathic Cystinosis. *Kidney Int.* **2021**, *100*, 1112–1123. [CrossRef] [PubMed]
24. Kalatzis, V.; Nevo, N.; Cherqui, S.; Gasnier, B.; Antignac, C.; Kalatzis, V.; Nevo, N.; Antignac, C.; Cherqui, S.; Gasnier, B.; et al. Molecular Pathogenesis of Cystinosis: Effect of CTNS Mutations on the Transport Activity and Subcellular Localization of Cystinosin. *Hum. Mol. Genet.* **2004**, *13*, 1361–1371. [CrossRef] [PubMed]
25. Cherqui, S.; Kalatzis, V.; Trugnan, G.; Antignac, C. The Targeting of Cystinosin to the Lysosomal Membrane Requires a Tyrosine-Based Signal and a Novel Sorting Motif*. *J. Biol. Chem.* **2001**, *276*, 13314–13321. [CrossRef] [PubMed]
26. Kalatzis, V.; Cordier, A.; Cochat, P.; Broyer, M.; Antignac, C.; Malades, N.; Bernard, C. Cystinosin, the Protein Defective in Cystinosis, Is a H+-Driven Lysosomal Cystine Transporter. *J. Am. Soc. Nephrol.* **2001**, *12*, 2170–2174. [CrossRef] [PubMed]
27. Guo, X.; Schmiege, P.; Assafa, T.E.; Wang, R.; Xu, Y.; Donnelly, L.; Fine, M.; Ni, X.; Jiang, J.; Millhauser, G.; et al. Structure and Mechanism of Human Cystine Exporter Cystinosin. *Cell* **2022**, *185*, 3739–3752.e18. [CrossRef] [PubMed]
28. Löbel, M.; Salphati, S.P.; El Omari, K.; Wagner, A.; Tucker, S.J.; Parker, J.L.; Newstead, S. Structural Basis for Proton Coupled Cystine Transport by Cystinosin. *Nat. Commun.* **2022**, *13*, 4845. [CrossRef] [PubMed]
29. Cheng, J.; Novati, G.; Pan, J.; Bycroft, C.; Žemgulyte, A.; Applebaum, T.; Pritzel, A.; Wong, L.H.; Zielinski, M.; Sargeant, T.; et al. Accurate Proteome-Wide Missense Variant Effect Prediction with AlphaMissense. *Science* **2023**, *381*, eadg7492. [CrossRef] [PubMed]
30. Jumper, J.; Evans, R.; Pritzel, A.; Green, T.; Figurnov, M.; Ronneberger, O.; Tunyasuvunakool, K.; Bates, R.; Žídek, A.; Potapenko, A.; et al. Highly Accurate Protein Structure Prediction with AlphaFold. *Nature* **2021**, *596*, 583–589. [CrossRef] [PubMed]
31. Wilmer, M.J.; Saleem, M.A.; Masereeuw, R.; Ni, L.; Van Der Velden, T.J.; Russel, F.G.; Mathieson, P.W.; Monnens, L.A.; Van Den Heuvel, L.P.; Levtchenko, E.N. Novel Conditionally Immortalized Human Proximal Tubule Cell Line Expressing Functional Influx and Efflux Transporters. *Cell Tissue Res.* **2010**, *339*, 449–457. [CrossRef] [PubMed]
32. Jamalpoor, A.; Van Gelder, C.A.G.H.; Yousef Yengej, F.A.; Zaal, E.A.; Berlingerio, S.P.; Veys, K.R.; Pou Casellas, C.; Voskuil, K.; Essa, K.; Ammerlaan, C.M.E.; et al. Cysteamine–Bicalutamide Combination Therapy Corrects Proximal Tubule Phenotype in Cystinosis. *EMBO Mol. Med.* **2021**, *13*, e13067. [CrossRef] [PubMed]
33. Besouw, M.; Van Den Heuvel, L.; Van Eijsden, R.; Bongaers, I.; Kluijtmans, L.; Dewerchin, M.; Levtchenko, E. Increased Human Dermal Microvascular Endothelial Cell Survival Induced by Cysteamine. *J. Inherit. Metab. Dis.* **2013**, *36*, 1073–1077. [CrossRef] [PubMed]
34. Iglesias, D.M.; El-Kares, R.; Taranta, A.; Bellomo, F.; Emma, F.; Besouw, M.; Levtchenko, E.; Toelen, J.; van den Heuvel, L.; Chu, L.L.; et al. Stem Cell Microvesicles Transfer Cystinosin to Human Cystinotic Cells and Reduce Cystine Accumulation in Vitro. *PLoS ONE* **2012**, *7*, e42840. [CrossRef] [PubMed]
35. Corallini, S.; Taranta, A.; Bellomo, F.; Palma, A.; Pastore, A.; Emma, F. Transcriptional and Post-Transcriptional Regulation of the CTNS Gene. *Pediatr. Res.* **2011**, *70*, 130–135. [CrossRef] [PubMed]
36. Van Looveren, D.; Giacomazzi, G.; Thiry, I.; Sampaolesi, M.; Gijsbers, R. Improved Functionality and Potency of next Generation BinMLV Viral Vectors toward Safer Gene Therapy. *Mol. Ther. Methods Clin. Dev.* **2021**, *23*, 51–67. [CrossRef] [PubMed]
37. Ibrahimi, A.; Vande Velde, G.; Reumers, V.; Toelen, J.; Thiry, I.; Vandeputte, C.; Vets, S.; Deroose, C.; Bormans, G.; Baekelandt, V.; et al. Highly Efficient Multicistronic Lentiviral Vectors with Peptide 2A Sequences. *Hum. Gene Ther.* **2009**, *20*, 845–860. [CrossRef] [PubMed]

38. Veys, K.; Berlingerio, S.P.; David, D.; Bondue, T.; Held, K.; Reda, A.; van den Broek, M.; Theunis, K.; Janssen, M.; Cornelissen, E.; et al. Urine-Derived Kidney Progenitor Cells in Cystinosis. *Cells* **2022**, *11*, 1245. [CrossRef] [PubMed]
39. Fehse, B.; Kustikova, O.S.; Bubenheim, M.; Baum, C. Pois(s)on—It's a Question of Dose. *Gene Ther.* **2004**, *11*, 879–881. [CrossRef] [PubMed]
40. Tordai, H.; Torres, O.; Csepi, M.; Padányi, R.; Lukács, G.L.; Hegedűs, T. Lightway Access to AlphaMissense Data That Demonstrates a Balanced Performance of This Missense Mutation Predictor. *bioRxiv* **2023**. [CrossRef]
41. Minton, K. Predicting Variant Pathogenicity with AlphaMissense. *Nat. Rev. Genet.* **2023**, *24*, 804. [CrossRef] [PubMed]
42. Zhang, P.; Bigio, B.; Rapaport, F.; Zhang, S.Y.; Casanova, J.L.; Abel, L.; Boisson, B.; Itan, Y. PopViz: A Webserver for Visualizing Minor Allele Frequencies and Damage Prediction Scores of Human Genetic Variations. *Bioinformatics* **2018**, *34*, 4307–4309. [CrossRef] [PubMed]
43. Shotelersuk, V.; Larson, D.; Anikster, Y.; Mcdowell, G.; Lemons, R.; Bernardini, I.; Guo, J.; Thoene, J.; Gahl, W.A. CTNS Mutations in an American-Based Population of Cystinosis Patients. *Am. J. Hum. Genet.* **1998**, *63*, 1352–1362. [CrossRef] [PubMed]
44. Midgley, J.P.; El-Kares, R.; Mathieu, F.; Goodyer, P. Natural History of Adolescent-Onset Cystinosis. *Pediatr. Nephrol.* **2011**, *26*, 1335–1337. [CrossRef] [PubMed]
45. Nevo, N.; Thomas, L.; Chhuon, C.; Andrzejewska, Z.; Lipecka, J.; Bailleux, A.; Edelman, A.; Antignac, C.; Guerrera, I.C.; Guillonneau, F.; et al. Impact of Cystinosin Glycosylation on Protein Stability by Differential Dynamic Stable Isotope Labeling by Amino Acids in Cell Culture (SILAC). *Mol. Cell. Proteomics* **2017**, *16*, 457–468. [CrossRef] [PubMed]
46. Braun, D.A.; Schueler, M.; Halbritter, J.; Gee, H.Y.; Porath, J.D.; Lawson, J.A.; Airik, R.; Shril, S.; Allen, S.J.; Stein, D.; et al. Whole Exome Sequencing Identifies Causative Mutations in the Majority of Consanguineous or Familial Cases with Childhood-Onset Increased Renal Echogenicity. *Kidney Int.* **2016**, *89*, 468–475. [CrossRef] [PubMed]
47. Cabrera-Serrano, M.; Junckerstorff, R.C.; Alisheri, A.; Pestronk, A.; Laing, N.G.; Weihl, C.C.; Lamont, P.J. Cystinosis Distal Myopathy, Novel Clinical, Pathological and Genetic Features. *Neuromuscul. Disord.* **2017**, *27*, 873–878. [CrossRef] [PubMed]
48. Savostyanov, K.V.; Pushkov, A.A.; Shchagina, O.A.; Maltseva, V.V.; Suleymanov, E.A.; Zhanin, I.S.; Mazanova, N.N.; Fisenko, A.P.; Mishakova, P.S.; Polyakov, A.V.; et al. Genetic Landscape of Nephropathic Cystinosis in Russian Children. *Front. Genet.* **2022**, *13*, 863157. [CrossRef] [PubMed]
49. Venkatarangan, V.; Zhang, W.; Yang, X.; Thoene, J.G.; Hahn, S.H.; Li, M. ER-Associated Degradation in Cystinosis Pathogenesis and the Prospects of Precision Medicine. *J. Clin. Investig.* **2023**, *133*, e169551. [CrossRef] [PubMed]
50. Thoene, J.; Lemons, R.; Anikster, Y.; Mullet, J.; Paelicke, K.; Lucero, C.; Gahl, W.; Schneider, J.; Shu, S.G.; Campbell, H.T. Mutations of CTNS Causing Intermediate Cystinosis. *Mol. Genet. Metab.* **1999**, *67*, 283–293. [CrossRef]
51. Zhang, J.; Johnson, J.L.; He, J.; Napolitano, G.; Ramadass, M.; Rocca, C.; Kiosses, W.B.; Bucci, C.; Xin, Q.; Gavathiotis, E.; et al. Cystinosin, the Small GTPase Rab11, and the Rab7 Effector RILP Regulate Intracellular Trafficking of the Chaperone-Mediated Autophagy Receptor LAMP2A. *J. Biol. Chem.* **2017**, *292*, 10328–10346. [CrossRef] [PubMed]
52. Andrzejewska, Z.; Nevo, N.; Thomas, L.; Chhuon, C.; Bailleux, A.; Chauvet, V.; Courtoy, P.J.; Chol, M.; Chiara Guerrera, I.; Antignac, C. Cystinosin Is a Component of the Vacuolar H+-ATPase-Ragulator-Rag Complex Controlling Mammalian Target of Rapamycin Complex 1 Signaling. *J. Am. Soc. Nephrol.* **2016**, *27*, 1678–1688. [CrossRef] [PubMed]
53. Kalatzis, V.; Cohen-Solal, L.; Cordier, B.; Frishberg, Y.; Kemper, M.; Nuutinen, E.M.; Legrand, E.; Cochat, P.; Antignac, C. Identification of 14 Novel CTNS Mutations and Characterization of Seven Splice Site Mutations Associated with Cystinosis. *Hum. Mutat.* **2002**, *20*, 439–446. [CrossRef] [PubMed]
54. Yeetong, P.; Tongkobpetch, S.; Kingwatanakul, P.; Deekajorndech, T.; Bernardini, I.M.; Suphapeetiporn, K.; Gahl, W.A.; Shotelersuk, V. Two Novel CTNS Mutations in Cystinosis Patients in Thailand. *Gene* **2012**, *499*, 323–325. [CrossRef] [PubMed]
55. Li, X.; Koudstaal, W.; Fletcher, L.; Costa, M.; van Winsen, M.; Siregar, B.; Inganäs, H.; Kim, J.; Keogh, E.; Macedo, J.; et al. Naturally Occurring Antibodies Isolated from PD Patients Inhibit Synuclein Seeding in Vitro and Recognize Lewy Pathology. *Acta Neuropathol.* **2019**, *137*, 825–836. [CrossRef] [PubMed]
56. Attard, M.; Jean, G.G.; Forestier, L.; Cherqui, S.S.; Van't Hoff, W.; Broyer, M.; Antignac, C.; Town, M. Severity of Phenotype in Cystinosis Varies with Mutations in the CTNS Gene: Predicted Effect on the Model of Cystinosin. *Hum. Mol. Genet.* **1999**, *8*, 2507–2514. [CrossRef] [PubMed]
57. Rupar, C.A.; Matsell, D.; Surry, S.; Siu, V. A G339R Mutation in the CTNS Gene Is a Common Cause of Nephropathic Cystinosis in the South Western Ontario Amish Mennonite Population. *J. Med. Genet.* **2001**, *38*, 615–616. [CrossRef] [PubMed]
58. Kiehntopf, M.; Schickel, J.; von der Gönne, B.; Koch, H.G.; Superti-Furga, A.; Steinmann, B.; Deufel, T.; Harms, E. Analysis of the CTNS Gene in Patients of German and Swiss Origin with Nephropathic Cystinosis. *Hum. Mutat.* **2002**, *20*, 237. [CrossRef] [PubMed]
59. Mason, S.; Pepe, G.; Dall'Amico, R.; Tartaglia, S.; Casciani, S.; Greco, M.; Bencivenga, P.; Murer, L.; Rizzoni, G.; Tenconi, R.; et al. Mutational Spectrum of the CTNS Gene in Italy. *Eur. J. Hum. Genet.* **2003**, *11*, 503–508. [CrossRef] [PubMed]
60. Macías-Vidal, J.; Rodés, M.; Hernández-Pérez, J.M.; Vilaseca, M.A.; Coll, M.J. Analysis of the CTNS Gene in 32 Cystinosis Patients from Spain. *Clin. Genet.* **2009**, *76*, 486–489. [CrossRef] [PubMed]
61. Soliman, N.A.; Elmonem, M.A.; van den Heuvel, L.; Abdel Hamid, R.H.; Gamal, M.; Bongaers, I.; Marie, S.; Levtchenko, E. Mutational Spectrum of the CTNS Gene in Egyptian Patients with Nephropathic Cystinosis. *JIMD Rep.* **2014**, *14*, 87. [CrossRef] [PubMed]

62. Sadeghipour, F.; Basiratnia, M.; Derakhshan, A.; Fardaei, M. Mutation Analysis of the CTNS Gene in Iranian Patients with Infantile Nephropathic Cystinosis: Identification of Two Novel Mutations. *Hum. Genome Var.* **2017**, *4*, 17038. [CrossRef] [PubMed]
63. Topaloglu, R.; Gulhan, B.; İnözü, M.; Canpolat, N.; Yilmaz, A.; Noyan, A.; Dursun, İ.; Gökçe, İ.; Gürgöze, M.K.; Akinci, N.; et al. The Clinical and Mutational Spectrum of Turkish Patients with Cystinosis. *Clin. J. Am. Soc. Nephrol.* **2017**, *12*, 1634–1641. [CrossRef] [PubMed]
64. Wilmer, M.J.; Emma, F.; Levtchenko, E.N. The Pathogenesis of Cystinosis: Mechanisms beyond Cystine Accumulation. *Am. J. Physiol.-Ren. Physiol.* **2010**, *299*, F905–F916. [CrossRef] [PubMed]
65. Demirsoy, S.; Martin, S.; Motamedi, S.; van Veen, S.; Holemans, T.; Van den Haute, C.; Jordanova, A.; Baekelandt, V.; Vangheluwe, P.; Agostinis, P. ATP13A2/PARK9 Regulates Endo-/Lysosomal Cargo Sorting and Proteostasis through a Novel PI(3, 5)P2-Mediated Scaffolding Function. *Hum. Mol. Genet.* **2017**, *26*, 1656–1669. [CrossRef] [PubMed]
66. Bellomo, F.; Corallini, S.; Pastore, A.; Palma, A.; Laurenzi, C.; Emma, F.; Taranta, A. Modulation of CTNS Gene Expression by Intracellular Thiols. *Free Radic. Biol. Med.* **2010**, *48*, 865–872. [CrossRef] [PubMed]
67. Donello, J.E.; Loeb, J.E.; Hope, T.J. Woodchuck Hepatitis Virus Contains a Tripartite Posttranscriptional Regulatory Element. *J. Virol.* **1998**, *72*, 5085–5092. [CrossRef] [PubMed]
68. Ruivo, R.; Bellenchi, G.C.; Chen, X.; Zifarelli, G.; Sagneá, C.; Debacker, C.C.; Pusch, M.; Supplisson, S.S.; Gasnier, B.; Sagné, C.; et al. Mechanism of Proton/Substrate Coupling in the Heptahelical Lysosomal Transporter Cystinosin. *Proc. Natl. Acad. Sci. USA* **2012**, *109*, E210–E217. [CrossRef]
69. Berquez, M.; Chen, Z.; Festa, B.P.; Krohn, P.; Keller, S.A.; Parolo, S.; Korzinkin, M.; Gaponova, A.; Laczko, E.; Domenici, E.; et al. Lysosomal Cystine Export Regulates MTORC1 Signaling to Guide Kidney Epithelial Cell Fate Specialization. *Nat. Commun.* **2023**, *14*, 3994. [CrossRef] [PubMed]
70. Ensinck, M.M.; Carlon, M.S. One Size Does Not Fit All: The Past, Present and Future of CF Causal Therapies. *Cells* **2022**, *11*, 1868. [CrossRef] [PubMed]
71. Helip-Wooley, A.; Park, M.A.; Lemons, R.M.; Thoene, J.G. Expression of CTNS Alleles: Subcellular Localization and Aminoglycoside Correction in Vitro. *Mol. Genet. Metab.* **2002**, *75*, 128–133. [CrossRef] [PubMed]
72. Brasell, E.J.; Chu, L.L.; El Kares, R.; Seo, J.H.; Loesch, R.; Iglesias, D.M.; Goodyer, P. The Aminoglycoside Geneticin Permits Translational Readthrough of the CTNS W138X Nonsense Mutation in Fibroblasts from Patients with Nephropathic Cystinosis. *Pediatr. Nephrol.* **2019**, *34*, 873–881. [CrossRef] [PubMed]
73. Brasell, E.J.; Chu, L.L.; Akpa, M.M.; Eshkar-Oren, I.; Alroy, I.; Corsini, R.; Gilfix, B.M.; Yamanaka, Y.; Huertas, P.; Goodyer, P. The Novel Aminoglycoside, ELX-02, Permits CTNSW138X Translational Read-through and Restores Lysosomal Cystine Efflux in Cystinosis. *PLoS ONE* **2019**, *14*, e0223954. [CrossRef] [PubMed]
74. European Rare Kidney Disease Reference Network. Available online: https://www.erknet.org/ (accessed on 26 January 2024).
75. RaDiCo-French National Programme on Rare Disease Cohorts. Available online: https://radico.fr/en/ (accessed on 26 January 2024).